Traveling-Wave Tubes

By J. R. PIERCE

[SECOND INSTALLMENT]

CHAPTER IV

FILTER-TYPE CIRCUITS

Synopsis of Chapter

ASIDE FROM HELICES, the circuits most commonly used in traveling-wave tubes are iterated or filter-type circuits, composed of linear arrays of coupled resonant slots or cavities.

Sometimes the geometry of such structures is simple enough so that an approximate field solution can be obtained. In other cases, the behavior of the circuits can be inferred by considering the behavior of lumped-circuit analogues, and the behavior of the circuits with frequency can be expressed with varying degrees of approximation in terms of parameters which can be computed or experimentally evaluated.

In this chapter the field approach will be illustrated for some very simple circuits, and examples of lumped-circuit analogues of other circuits will be given. The intent is to present methods of analyzing circuits rather than particular numerical results, for there are so many possible configurations that a comprehensive treatment would constitute a book in itself.

Readers interested in a wider and more exact treatment of field solutions are referred to the literature.[1,2]

The circuit of Fig. 4.1 is one which can be treated by field methods. This "corrugated waveguide" type of circuit was first brought to the writer's attention by C. C. Cutler. It is composed of a series of parallel equally spaced thin fins of height h projecting normal to a conducting plane. The case treated is that of propagation of a transverse magnetic wave, the magnetic field being parallel to the length of the fins. It is assumed that the spacing ℓ is small compared with a wavelength. In Fig. 4.2, βh is plotted vs. $\beta_0 h$. Here β is the phase constant and $\beta_0 = \omega/c$ is a phase constant corresponding to the velocity of light.

[1] E. L. Chu and W. W. Hansen, "The Theory of Disk-Loaded Wave Guides," *Journal of Applied Physics*, Vol. 18, pp. 999–1008, Nov. 1947.

[2] L. Brillouin, "Wave Guides for Slow Waves," *Journal of Applied Physics*, Vol. 19, pp. 1023–1041, Nov. 1948.

For small values of $\beta_0 h$, that is, at low frequencies, very nearly $\beta = \beta_0$; that is, the phase velocity is very near to the velocity of light. The field decays slowly away from the circuit. The longitudinal electric field is small compared with the transverse electric field. In fact, as the frequency approaches zero, the wave approaches a transverse electromagnetic wave traveling with the speed of light.

At high frequencies the wave falls off rapidly away from the circuit, and the transverse and longitudinal components of electric field are almost equal. The wave travels very slowly. As the wavelength gets so short that the spacing ℓ approaches a half wavelength ($\beta\ell = \pi$) the simple analysis given is no longer valid. Actually, $\beta\ell = \pi$ specifies a cutoff frequency; the circuit behaves as a lowpass filter.

Figure 4.3 shows two opposed sets of fins such as those of Fig. 4.1. Such a circuit propagates two modes, a transverse mode for which the longitudinal electric field is zero at the plane of symmetry and a longitudinal mode for which the transverse electric field is zero at the plane of symmetry.

At low frequencies, the longitudinal mode corresponds to the wave on a loaded transmission line. The fins increase the capacitance between the conducting planes to which they are attached but they do not decrease the inductance. Figure 4.6 shows βh vs. $\beta_0 h$ for several ratios of fin height, h, to half-separation, d. The greater is h/d, the slower is the wave (the larger is β/β_0).

The longitudinal mode is like a transverse magnetic waveguide mode; it propagates only at frequencies above a cutoff frequency, which increases as h/d is increased. Figure 4.7 shows βh vs. $\beta_0 h = (\omega/c)h$ for several values of h/d. The cutoff, for which $\beta\ell = \pi$, occurs for a value of $\beta_0 h$ less than $\pi/2$. Thus, we see that the longitudinal mode has a band pass characteristic. The behavior of the longitudinal mode is similar to that of a longitudinal mode of the washer-loaded waveguide shown in Fig. 4.8. The circuit of Fig. 4.8 has been proposed for use in traveling-wave tubes.

The transverse mode of the circuit of Fig. 4.3 can also exist in a circuit consisting of strips such as those of Fig. 4.1 and an opposed conducting plane, as shown in Fig. 4.5. This circuit is analogous in behavior to the disk-on-rod circuit of Fig. 4.9. The circuit of Fig. 4.5 may be thought of as a loaded parallel strip line. That of Fig. 4.9 may be thought of as a loaded coaxial line.

Wave-analysis makes it possible to evaluate fairly accurately the transmission properties of a few simple structures. However, iterated or repeating structures have certain properties in common: the properties of filter networks.

For instance, a mode of propagation of the loaded waveguide of Fig. 4.10 or of the series of coupled resonators of Fig. 4.11 can be represented accurately at a single frequency by the ladder networks of Fig. 4.12. Further,

if suitable lumped-admittance networks are used to represent the admittances B_1 and B_2, the frequency-dependent behavior of the structures of Figs. 4.10 and 4.11 can be approximated.

It is, for instance, convenient to represent the shunt admittances B_2 and the series admittances B_1 in terms of a "longitudinal" admittance B_L and a "transverse" admittance B_T. B_L and B_T are admittances of shunt resonant circuits, as shown in Fig. 4.15, where their relation to B_1 and B_2 and approximate expressions for their frequency dependence are given. The resonant frequencies of B_L and B_T, that is, ω_L and ω_T, have simple physical meanings. Thus, in Fig. 4.10, ω_L is the frequency corresponding to equal and opposite voltages across successive slots, that is, the π mode frequency. ω_T is the frequency corresponding to zero slot voltage and no phase change along the filter, that is, the zero mode frequency.

If ω_L is greater than ω_T, the phase characteristic of this lumped-circuit analogue is as shown in Fig. 4.17. The phase shift is zero at the lower cutoff frequency ω_T and rises to π at the upper cutoff frequency ω_L. If ω_T is greater than ω_L, the phase shift starts at $-\pi$ at the lower cutoff frequency ω_L and rises to zero at the upper cutoff frequency ω_T, as shown in Fig. 4.19. In this case the phase velocity is negative. Figure 4.20 shows a measure of $(E^2/\beta^2 P)$ plotted vs. ω for $\omega_L > \omega_T$. This impedance parameter is zero at ω_T and rises to infinity at ω_L.

The structure of Fig. 4.11 can be given a lumped-circuit equivalent in a similar manner. In this case the representation should be quite accurate. We find that ω_L is always greater than ω_T and that one universal phase curve, shown in Fig. 4.27, applies. A curve giving a measure of $(E^2/\beta^2 P)$ vs. frequency is shown in Fig. 4.28. In this case the impedance parameter goes to infinity at both cutoff frequencies.

The electric field associated with iterated structures does not vary sinusoidally with distance but it can be analyzed into sinusoidal components. The electron stream will interact strongly with the circuit only if the electron velocity is nearly equal to the phase velocity of one of these field components. If θ is the phase shift per section and L is the section length, the phase constant β_m of a typical component is

$$\beta_m = (\theta + 2m\pi)/L$$

where m is a positive or negative integer. The field component for which $m = 0$ is called the fundamental; for other values of m the components are called *spatial harmonics*. Some of these components have negative phase velocities and some have positive phase velocities.

The peak field strength of any field component may be expressed

$$E = -M(V/L)$$

Here V is the peak gap voltage, L is the section spacing and M is a function of β (or β_m) and of various dimensions. For the electrode systems of Figs.

4.29, 4.30, 4.31 and 4.32 M is given by (4.69), (4.71), (4.72) and (4.73), respectively.

The factor M may be indifferently regarded as a factor by which we multiply the a-c beam current to give the induced current at the gap, or, as a factor by which we multiply the gap voltage in obtaining the field. We can go further, evaluate $E^2/\beta^2 P$ in terms of gap voltage, and use $M^2 I_0$ as the effective current, or we can use the current I_0 and take the effective field in the impedance parameter as

$$E^2 = M^2(V/\ell)^2$$

It is sometimes desirable to make use of a spatial harmonic ($m \neq 0$) instead of a fundamental, usually to (1) allow a greater resonator spacing (2) to obtain a positive phase velocity when the fundamental has a negative phase velocity (3) to obtain a phase curve for which the phase angle is nearly a constant times frequency; that is, a phase curve for which the group velocity does not change much with frequency and hence can be matched by the electron velocity over a considerable frequency range. Figure 4.33 shows how $\theta + 2\pi$ (the phase shift per section for $m = 1$) can be nearly a constant times ω even when θ is not.

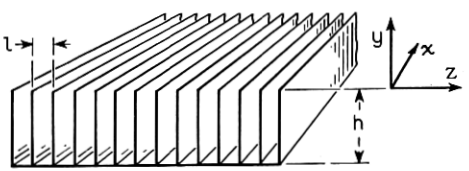

Fig. 4.1—A corrugated or finned circuit with filter-like properties.

4.1 Field Solutions

An approximate field analysis will be made for two very simple two-dimensional structures. The first of these, which is shown in Fig. 4.1, is empty space for $y > 1$ and consists of very thin conducting partitions in the y direction from $y = 0$ to $y = -h$; the partitions are connected together by a conductor in the z direction at $y = -h$. These conducting partitions are spaced a distance ℓ apart in the z direction. The structure is assumed to extend infinitely in the $+x$ and $-x$ directions.

In our analysis we will initially assume that the wavelength of the propagated wave is long compared with ℓ. In this case, the effect of the partitions is to prevent the existence of any y component of electric field below the z axis, and the conductor at $y = -h$ makes the z component of electric field zero at $y = -z$.

In some perfectly conducting structures the waves propagated are either transverse electric (no electric field component in the direction of propagation, that is, z direction) or transverse magnetic (no magnetic field com-

ponent in the z direction). We find that for the structure under consideration there is a transverse magnetic solution. We can take it either on the basis of other experience or as a result of having solved the problem that the correct form for the x component of magnetic field for $y > 0$ is

$$H_x = H_0 e^{(-\gamma y - j\beta z)} \tag{4.1}$$

Expressing the electric field in terms of the curl of the magnetic field, we have

$$j\omega\epsilon E_x = \frac{\partial Hz}{\partial y} - \frac{\partial Hy}{\partial z} = 0$$

$$j\omega\epsilon E_y = \frac{\partial Hx}{dz} - \frac{\partial Hz}{\partial x} \tag{4.2}$$

$$E_y = -\frac{\beta}{\omega\epsilon} H_0 e^{(-\gamma y - j\beta z)} \tag{4.3}$$

$$j\omega\epsilon E_z = \frac{\partial Hy}{\partial x} - \frac{\partial Hx}{\partial y} \tag{4.4}$$

$$E_z = -j\frac{\gamma}{\omega\epsilon} H_0 e^{(-\gamma y - j\beta z)} \tag{4.5}$$

We can in turn express H_x in terms of E_y and E_z

$$-j\omega\mu H_x = \frac{\partial Ez}{\partial y} - \frac{\partial Ey}{\partial z} \tag{4.6}$$

This leads to the relation

$$\beta^2 - \gamma^2 = \omega^2\mu\epsilon \tag{4.7}$$

Now, $1/\sqrt{\mu\epsilon}$ is the velocity of light, and ω divided by the velocity of light has been called β_0, so that

$$\beta^2 - \gamma^2 = \beta_0^2 \tag{4.8}$$

Between the partitions, the field does not vary in the z direction. In any space between from $y = 0$ to $y = -h$, the appropriate form for the magnetic field is

$$H_x = H_0 \frac{\cos \beta_0(y + h)}{\cos \beta_0 h} \tag{4.9}$$

From this we obtain by means of (4.4)

$$E_z = -\frac{j\beta_0}{\omega\epsilon} H_0 \frac{\sin \beta_0(y + h)}{\cos \beta_0 h} \tag{4.10}$$

Application of (4.6) shows that this is correct.

Now, at $y = 0$ we have just above the boundary

$$E_z = -j \frac{\gamma}{\omega\epsilon} H_0 e^{-j\beta z} \tag{4.11}$$

The fields in the particular slot just below the boundary will be in phase with these (we specify this by adding a factor exp $-j\beta z$ to 4.10) and hence will be

$$E_z = -\frac{j\beta_0}{\omega\epsilon} H_0 e^{-j\beta z} \tan \beta_0 h \tag{4.12}$$

From (4.11) and (4.12) we see that we must have

$$\beta_0 h \tan \beta_0 h = \gamma h \tag{4.13}$$

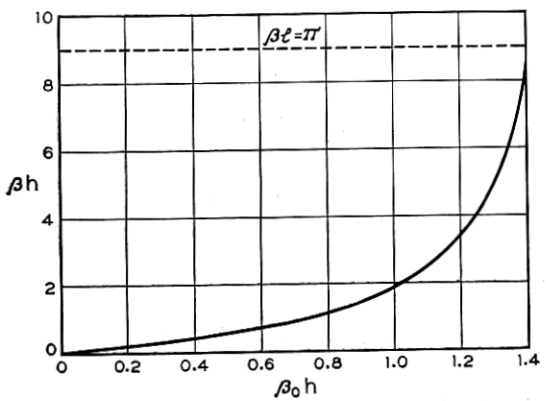

Fig. 4.2—The approximate variation of the phase constant β with frequency (proportional to $\beta_0 h$) for the circuit of Fig. 4.1. The curve is in error as $\beta\ell$ approaches π, and there is a cutoff at $\beta\ell = \pi$.

Using (4.8), we obtain

$$\beta h = \frac{\pm\beta_0 h}{\cos \beta_0 h} \tag{4.14}$$

In Fig. 4.2, βh has been plotted vs $\beta_0 h$, which is, of course, proportional to frequency. This curve starts out as a straight line, $\beta = \beta_0$; that is, for low frequencies the speed is the speed of light. At low frequencies the field falls off slowly in the y direction, and as the frequency approaches zero we have essentially a plane electromagnetic wave. At higher frequencies, $\beta > \beta_0$, that is, the wave travels with less than the speed of light, and the field falls off rapidly in the y direction. According to (4.14), β goes to infinity at $\beta_0 h = \pi/2$.

As a matter of fact, the match between the fields assumed above and below the boundary becomes increasingly bad as $\beta\ell$ becomes larger. The most rapid

alteration we can have below the boundary is one in which fields in alternate spaces follow a $+, -, +, -$ pattern. Thus, the rapid variations of field above the boundary predicted by (4.14) for values of $\beta_0 h$ which make $\beta \ell$ greater than π cannot be matched below the boundary. The frequency at which $\beta \ell = \pi$ constitutes the cutoff frequency of the structure regarded as a filter. There is another pass band in the region $\pi < \beta_0 h < 3\pi/2$, in which the ratio of E to H below the boundary has the same sign as the ratio of E to H above the boundary.

A more elaborate matching of fields would show that our expression is considerably in error near cutoff. This matter will not be pursued here; the behavior of filters near cutoff will be considered in connection with lumped circuit representations.

We can obtain the complex power flow P by integrating the Poynting vector over a plane normal to the z direction in the region $y > 0$. Let us consider the power flow over a depth W normal to the plane of the paper. Then

$$P = \frac{1}{2} \int_0^\infty \int_0^W (E_x H_y^* - E_y H_x^*) \, dx \, dy \tag{4.15}$$

Using (4.1) and (4.3), we obtain

$$\begin{aligned} P &= \frac{W}{2} \int_0^\infty \frac{\beta H_0^2}{\omega \epsilon} e^{-2\gamma y} \, dy \\ P &= \frac{1}{4} \frac{H_0^2 \beta W}{\omega \epsilon \gamma} \end{aligned} \tag{4.16}$$

We will express this in terms of E the magnitude of the z component of the field at $y = 0$, which, according to (4.5), is

$$E = \frac{\gamma}{\omega \epsilon} H_0 \tag{4.17}$$

We will also note that

$$\begin{aligned} \omega \epsilon &= \omega \sqrt{\mu \epsilon} / \sqrt{\mu / \epsilon} \\ &= (\omega / c) / \sqrt{\mu / \epsilon} = \beta_0 / \sqrt{\mu / \epsilon} \end{aligned} \tag{4.18}$$

and that

$$\sqrt{\mu / \epsilon} = 377 \text{ ohms} \tag{4.19}$$

By using (4.17)–(4.18) in connection with (4.16), we obtain

$$E^2 / \beta^2 P = (4 / \beta_0 W)(\gamma / \beta)^3 \sqrt{\mu / \epsilon} \tag{4.20}$$

We notice that this impedance is very small for low frequencies, at which

the velocity of the wave is high, and the field extends far in the y direction and becomes higher at high frequencies, where the velocity is low and the field falls off rapidly.

We will next consider a symmetrical array of two opposed sets of slots (Fig. 4.3) similar to that shown in Fig. 4.1. Two modes of propagation will be of interest. In one the field is symmetrical about the axis of physical symmetry, and in the other the fields at positions of physical symmetry are equal and opposite.

In writing the equations, we need consider only half of the circuit. It is convenient to take the z axis along the boundary, as shown in Fig. 4.4.

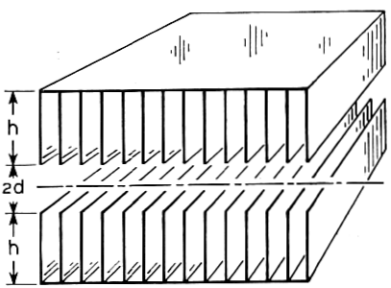

Fig. 4.3—A double finned structure which will support a transverse mode (no longitudinal electric field on axis) and a longitudinal mode (no transverse electric field on axis).

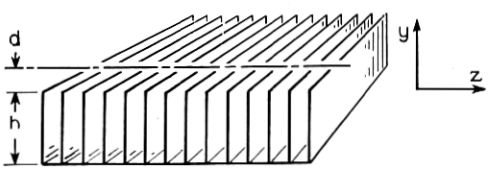

Fig. 4.4—The coordinates used in connection with the circuit of Fig. 4.3.

This puts the axis of symmetry at $y = +d$, and the slots extend from $y = 0$ to $y = -h$.

For negative values of y, (4.9), (4.10), (4.12) hold.

Let us first consider the case in which the fields above are opposite to the fields below. This also corresponds to waves in a series of slots opposite a conducting plane, as shown in Fig. 4.5. In this case the appropriate form of the magnetic field above the boundary is

$$H_x = H_0 \frac{\cosh \gamma(d - y)}{\cosh \gamma d} e^{-j\beta z} \tag{4.21}$$

From Maxwell's equations we then find

$$E_y = -\frac{\beta}{\omega\epsilon} H_0 \frac{\cosh \gamma(d - y)}{\cosh \gamma d} e^{-j\beta z} \tag{4.22}$$

$$E_z = -j\frac{\gamma}{\omega\epsilon} H_0 \frac{\sinh \gamma(d - y)}{\cosh \gamma d} e^{-j\beta z} \tag{4.23}$$

$$\beta_0^2 = \beta^2 - \gamma^2 \tag{4.24}$$

At $y = 0$ we have from (4.23) and (4.12)

$$E_z = -j\frac{\gamma}{\omega\epsilon} H_0 e^{-j\beta z} \tanh \gamma d \tag{4.25}$$

$$E_z = -j\frac{\beta_0}{\omega\epsilon} H_0 e^{-j\beta z} \tan \beta_0 h \tag{4.12}$$

Hence, we must have

$$\gamma h \tanh ((d/h)\gamma h) = \beta_0 h \tan \beta_0 h \tag{4.26}$$

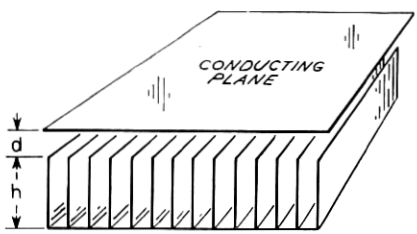

Fig. 4.5—The transverse mode of the circuit of Fig. 4.3 exists in this circuit also.

Here we have added parameter, (d/h). For any value of d/h, we can obtain γh vs $\beta_0 h$; and we can obtain βh in terms of γh by means of 4.24

$$\beta h = ((\gamma h)^2 + (\beta_0 h)^2)^{1/2} \tag{4.27}$$

We see that for small values of $\beta_0 h$ (low frequencies)

$$\gamma^2 = (h/d)\,\beta_0^2 \tag{4.28}$$

$$\beta = \beta_0 \left(\frac{h + d}{d}\right)^{1/2} \tag{4.29}$$

If we examine Fig. 4.5, to which this applies, we find (4.28) easy to explain. At low frequencies, the magnetic field is essentially constant from $y = d$ to $y = -h$, and hence the inductance is proportional to the height $h + d$. The electric field will, however, extend only from $y = 0$ to $y = d$; hence the capacitance is proportional to $1/d$. The phase constant is proportional to $\sqrt{LC}$, and hence (4.29). At higher frequencies the electric and magnetic fields vary with y and (4.29) does not hold.

We see that (4.26) predicts infinite values of γ for $\beta h = \pi/2$. As in the previous cases, cutoff occurs at $\beta \ell = \pi$.

As an example of the phase characteristic of the circuit, βh from (4.26) and (4.27) is plotted vs $\beta_0 h$ for $h/d = 0, 10, 100$ in Fig. 4.6. The curve for $h/d = 0$ is of course the same as Fig. 4.2.

If we integrate Poynting's vector from $y = 0$ to $y = d$ and for a distance W in the x direction, and multiply by 2 to take the power flow in the other half of the circuit into account, we obtain

$$E^2/\beta^2 P = (2/\beta_0 W)(\gamma/\beta)^3 \left(\frac{\sinh^2 \gamma d}{\sinh \gamma d \cosh \gamma d + \gamma d} \right) \sqrt{\mu/\epsilon} \quad (4.30)$$

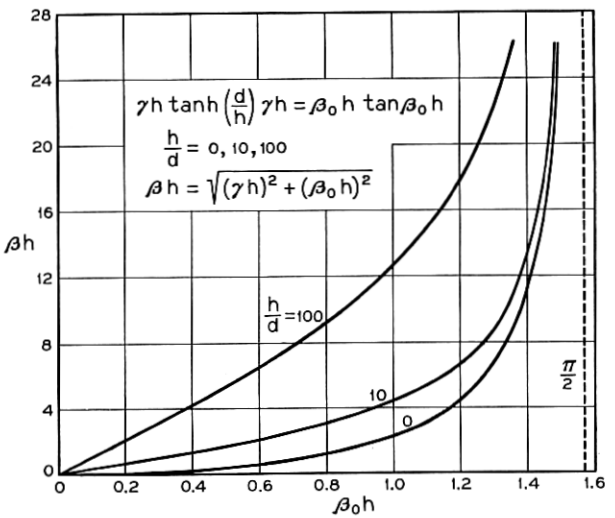

Fig. 4.6—The variation of β with frequency (proportional to $\beta_0 h$) for the transverse mode of the circuit of Fig. 4.3. Again, the curves are in error near the cutoff at $\beta \ell = \pi$.

At very low frequencies, at which (4.28) and (4.29) hold, we have

$$\begin{aligned} E^2/\beta^2 P &= (\gamma^4/\beta_0 \beta^3)(d/W) \sqrt{\mu/\epsilon} \\ E^2/\beta^2 P &= (h/d)^{1/2} (1 + d/h)^{3/2} (d/W) \sqrt{\mu/\epsilon} \end{aligned} \quad (4.31)$$

At high frequencies, for which γd is large, (4.30) approaches $\frac{1}{2}$ of the value given by (4.20). There is twice as much power because there are two halves to the circuit.

Let us now consider the case in which the field is symmetrical and E_z does not go to zero on the axis. In this case the appropriate field for $y > 0$ is

$$H_x = H_0 \frac{\sinh \gamma(d - y)}{\sinh \gamma d} e^{-j\beta z} \quad (4.32)$$

Proceeding as before, we find

$$\frac{\gamma h}{\tanh\left((d/h)\,\gamma h\right)} = \beta_0 h \tan \beta_0 h \tag{4.33}$$

We see that, in this case, for small values of γh we have

$$\beta_0 h \tanh \beta_0 h = h/d \tag{4.33a}$$

There is no transmission at all for frequencies below that specified by (4.33). As the frequency is increased above this lower cutoff frequency, γh and hence βh increase, and approach infinity at $\beta_0 h = \pi/2$. Actually, of course, the upper cutoff occurs at $\beta \ell = \pi$. In Fig. 4.7 βh is plotted vs $\beta_0 h$ for $h/d = 0$,

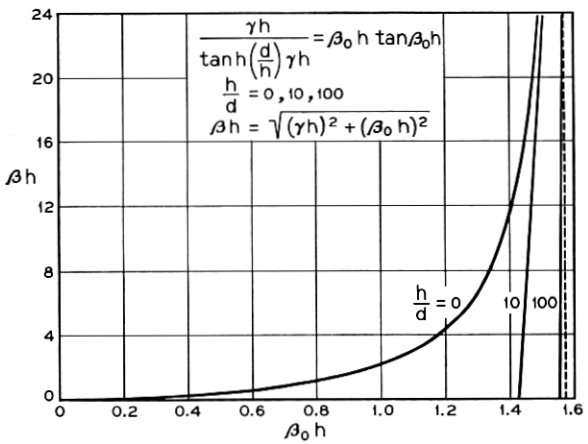

Fig. 4.7—The variation of β with frequency (proportional to $\beta_0 h$) for the longitudinal mode of the circuit of Fig. 4.3. This mode has a band pass characteristic; the band narrows as the opening of width 2d is made small compared with the fin height. Again, the curves are in error near the upper cutoff at $\beta \ell = \pi$.

10, 100. This illustrates how the band is narrowed as the opening between the slots is decreased.

By the means used before we obtain

$$E^2/\beta^2 P = (2/\beta_0 W)(\gamma/\beta)^3 \left(\frac{\cosh^2 \gamma d}{\sinh \gamma d \cosh \gamma d - \gamma d}\right) \sqrt{\mu/\epsilon} \tag{4.34}$$

We see that this goes to infinity at $\gamma d = 0$. For large values of γd it becomes the same as (4.30).

4.2 Practical Circuits

Circuits have been proposed or used in traveling-wave tubes which bear a close resemblance to those of Figs. 4.1, 4.3, 4.5 and which have very similar

properties[3]. Thus Field[4] describes an apertured disk structure (Fig. 4.8) which has band-pass properties very similar to the symmetrical mode of the circuit of Fig. 4.3. In this case there is no mode similar to the other mode, with equal and opposite fields in the two halves. Field also shows a disk-on-rod structure (Fig. 4.9) and describes a tube using it. This structure has low-

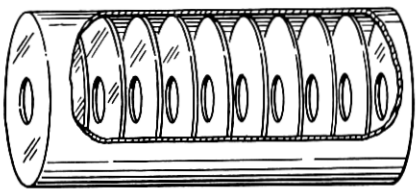

Fig. 4.8—This loaded waveguide circuit has band-pass properties similar to those of Fig. 4.7.

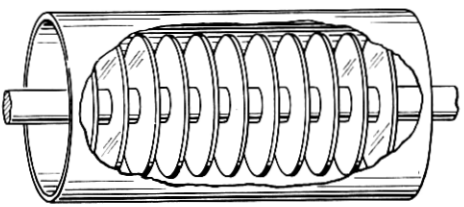

Fig. 4.9—This disk-on-rod circuit has properties similar to those of Fig. 4.6.

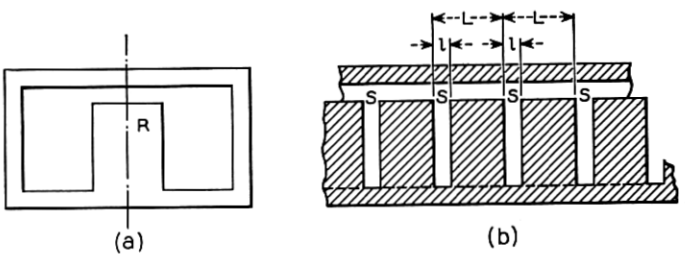

Fig. 4.10—A circuit consisting of a ridged waveguide with transverse slots or resonators in the ridge.

pass properties very similar to those of the circuit of Fig. 4.5, which are illustrated in Fig. 4.6.

Figure 4.10 shows a somewhat more complicated circuit. Here we have a rectangular waveguide, shown end on in *a* of Fig. 4.10, loaded by a longitudinal ridged portion *R*. In *b* of Fig. 4.10 we have a longitudinal cross sec-

[3] F. B. Llewellyn, *U. S. Patents* 2,367,295 and 2,395,560.

[4] Lester M. Field, "Some Slow-Wave Structures for Traveling-Wave Tubes," *Proc. I.R.E.*, Vol. 37, pp. 34–40, Jan. 1949.

tion, showing regularly spaced slots S cut in the ridge R. The slots S may be thought of as resonators.

Figure 4.11 shows in cross section a circuit made of a number of axially symmetrical reentrant resonators R, coupled by small holes H which act as inductive irises.

It would be very difficult to apply Maxwell's equations directly in deducing the performance of the structures shown in Figs. 4.10 and 4.11. Moreover, it is apparent that we can radically change the performance of

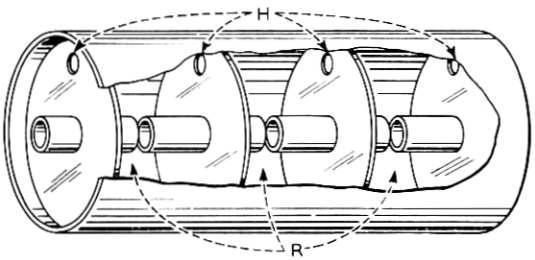

Fig. 4.11—A circuit consisting of a number of resonators inductively coupled by means of holes.

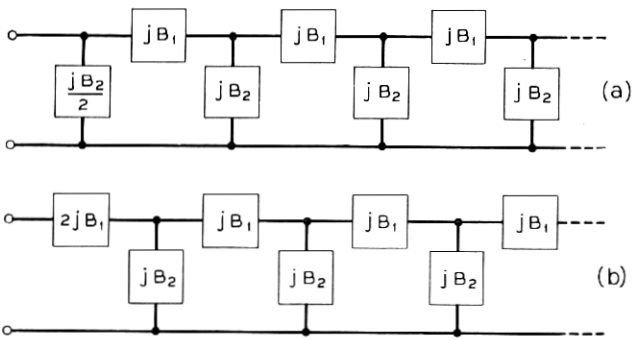

Fig. 4.12—Ladder networks terminated in π (above) and T (below) half sections. Such networks can be used in analyzing the behavior of circuits such as those of Figs. 4.10 and 4.11.

such structures by minor physical alterations as, by changing the iris size, or by using resonant irises in the circuit of Fig. 4.11, for instance.

As a matter of fact, it is not necessary to solve Maxwell's equations afresh each time in order to understand the general properties of these and other circuits.

4.3 Lumped Iterated Analogues

Consider the ladders of lossless admittances or susceptances shown in Fig. 4.12. Susceptances rather than reactances have been chosen because the

elements we shall most often encounter are shunt resonant near the frequencies considered; their susceptance is near zero and changing slowly but their reactance is near infinity.

If these ladders are continued endlessly to the right (or terminated in a reflectionless manner) and if a signal is impressed on the left-hand end, the voltages, currents and fields at corresponding points in successive sections will be in the ratio exp(-Γ) so that we can write the voltages,

$$V_n = V_0 e^{-n\Gamma} \tag{4.35}$$

If the admittances Y_1 and Y_2 are pure susceptances (lossless reactors), Γ is either purely real (an exponential decay with distance) or purely imaginary (a pass band). In this case Γ is usually replaced by $j\beta$. In order to avoid confusion of notation, we will use $j\theta$ instead, and write for the lossless case in the pass band

$$V_n = V_0 e^{-jn\theta} \tag{4.35a}$$

Thus, θ is the phase lag in radians in going from one section to the next. In terms of the susceptances,*

$$\cos\theta = 1 + B_2/2B_1 \tag{4.36}$$

We will henceforward assume that all elements are lossless.

Two characteristic impedances are associated with such iterated networks. If the network starts with a shunt susceptance $B_1/2$, as in *a* of Fig. 4.12, then we see the mid-shunt characteristic impedance K_π

$$K_\pi = 2(-B_2(B_2 + 4B_1))^{-1/2} \tag{4.37}$$

If the network starts with a series susceptance $2B_1$ we see the mid-series characteristic impedance K_T

$$K_T = \pm(1/2B_1)(-B_2 + 4B_1)/B_2)^{1/2} \tag{4.38}$$

Here the sign is chosen to make the impedance positive in the pass band.

When such networks are used as circuits for a traveling-wave tube, the voltage acting on the electron stream may be the voltage across B_2 or the voltage across B_1 or the voltage across some capacitive element of B_2 or B_1. We will wish to relate this peak voltage V to the power flow P. If the voltage across B_2 acts on the electron stream

$$V^2/P = 2K_\pi \tag{4.39}$$

If the voltage across Y_1 acts on the electron stream

$$V = I/jB_1$$

* The reader can work such relations out or look them up in a variety of books or handbooks. They are in Schelkunoff's Electromagnetic Waves.

where I is the current in B_1

$$P = |I^2| K_T/2$$

and hence

$$V^2/P = 2/B_1^2 K_T \tag{4.40}$$

$$V^2/P = -4(B_2/B_1)(-B_2(B_2 + 4B_1))^{-1/2} \tag{4.41}$$

$$V^2/P = -2(B_2/B_1)K_\pi \tag{4.42}$$

Here the sign has been chosen so as to make V^2/P positive in the pass band.

Let us now consider as an example the structure of Fig. 4.10. We see that two sorts of resonance are possible. First, if all the slots are shorted, or if no voltage appears between them, we can have a resonance in which the field between the top of the ridge R and the top of the waveguide is constant

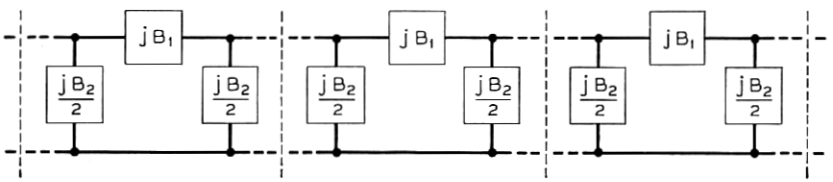

Fig. 4.13—A ladder network broken up into π sections.

all along the length, and corresponds to the cutoff frequency of the ridged waveguide. There are no longitudinal currents (or only small ones near the slots S) and hence there is no voltage across the slots and their admittance (the slot depth, for instance) does not affect the frequency of this resonance. Looking at Fig. 4.12, we see that this corresponds to a condition in which all shunt elements are open, or $B_2 = 0$. We will call the frequency of this resonance ω_T, the T standing for transverse.

There is another simple resonance possible; that in which the fields across successive slots are equal and opposite. Looking at Fig. 4.12, we see that this means that equal currents flow into each shunt element from the two series elements which are connected to it. We could, in fact, divide the network up into unconnected π sections, associating with each series element of susceptance B_1 half of the susceptance of a shunt element, that is, $B_2/2$, at each end, as shown in Fig. 4.13, without affecting the frequency of this resonance. This resonance, then, occurs at the frequency ω_L (L for longitudinal) at which

$$B_1 + B_2/4 = 0. \tag{4.43}$$

We have seen that the transverse resonant frequency, ω_T, has a clear meaning in connection with the structure of Fig. 4.10; it is (except for small

errors due to stray fields near the slots) the cutoff frequency of the waveguide without slots. Does the longitudinal frequency ω_L have a simple meaning?

Suppose we make a model of one section of the structure, as shown in Fig. 4.14. Comparing this with *b* of Fig. 4.10, we see that we have included the section of the ridged portion between two slots, and one half of a slot at each end, and closed the ends off with conducting plates *C*. The resonant frequency of this model is ω_L, the longitudinal resonant frequency defined above.

We will thus liken the structure of Fig. 4.10 to the filter network of Fig.

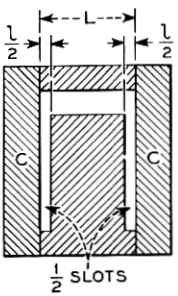

Fig. 4.14—A section which will have a resonant frequency corresponding to that for π radians phase shift per section in the circuit of Fig. 4.10.

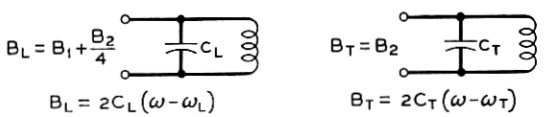

Fig. 4.15—The approximate variation with frequency (over a narrow band) of the longitudinal (B_L) transverse (B_T) susceptances of a filter network.

4.12, and express the susceptances B_1 and B_2 in terms of two susceptances B_T and B_L associated with the transverse and longitudinal resonances and defined below

$$B_T = B_2 \tag{4.44}$$

$$B_L = B_1 + B_2/4 \tag{4.45}$$

At the transverse resonant frequency ω_T, $B_T = 0$, and at the longitudinal resonant frequency ω_L, $B_L = 0$. So far, the lumped-circuit representation of the structure of Fig. 4.14 can be considered exact in the sense that at any frequency we can assign values to B_T and B_L which will give the correct values for θ and for V^2/P for the voltage across either the shunt or the series elements (whichever we are interested in).

We will go further and assume that near resonances these values of B_T and B_L behave like the admittances of shunt resonant circuits, as indicated in Fig. 4.15. Certainly we are right by our definition in saying that $B_T = 0$ at ω_T, and $B_L = 0$ at ω_L. We will assume near these frequencies a linear variation of B_T and B_L with frequency, which is very nearly true for shunt resonant circuits near resonance*

$$B_T = 2C_T(\omega - \omega_T) \tag{4.46}$$

$$B_L = 2C_L(\omega - \omega_L) \tag{4.47}$$

Here C_T can mean twice the peak stored electric energy per section length for unit peak voltage between the top of the guide and the top of the ridge R when the structure resonates in the transverse mode, and C_L can mean twice the stored energy per section length L for unit peak voltage across the top

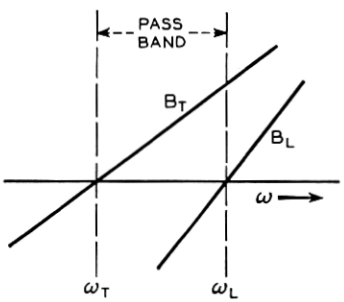

Fig. 4.16—Longitudinal and transverse susceptances which give zero radians phase shift at the lower cutoff ($\omega = \omega_T$) and π radians phase shift at the upper cutoff ($\omega = \omega_L$).

of the slot when the structure resonates in the longitudinal mode.

In terms of B_T and B_L, expression (4.36) for the phase angle θ becomes

$$\cos\theta = \frac{4B_L + B_T}{4B_L - B_T} \tag{4.48}$$

We see immediately that for real values of θ ($\cos\theta \leq 1$), B_T and B_L must have opposite signs, making the denominator greater than the numerator.

Figure 4.16 shows one possible case, in which $\omega_T < \omega_L$. In this case the pass band (θ real) starts at the lower cutoff frequency $\omega = \omega_T$ at which B_T is zero, $\cos\theta = 1$ (from (4.48)) and $\theta = 0$, and extends up to the upper cutoff frequency $\omega = \omega_L$ at which $B_L = 0$, $\cos\theta = -1$ and $\theta = \pi$.

* In case the filter has a large fractional bandwidth, it may be worth while to use the accurate lumped-circuit forms

$$B_T = \omega_T C_T(\omega/\omega_T - \omega_T/\omega) \tag{4.46a}$$

$$B_L = \omega_L C_L(\omega/\omega_L - \omega_L/\omega) \tag{4.46b}$$

The shape of the phase curves will depend on the relative rates of variation of B_T and B_L with frequency. Assuming the linear variations with frequency of (4.46) and (4.47) the shapes can be computed. This has been done for $C_L/C_T = 1, 3, 10$ and the results are shown in Fig. 4.17.

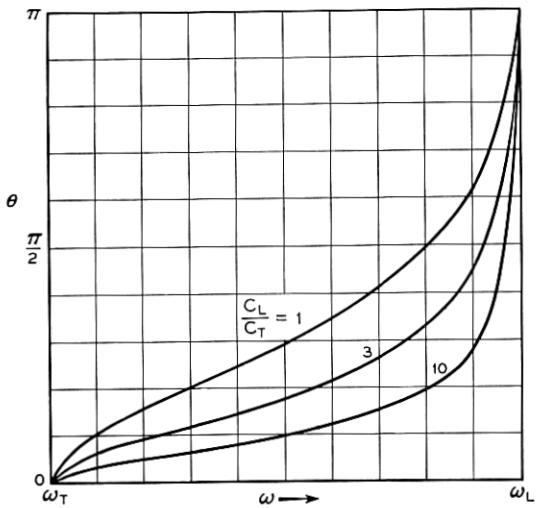

Fig. 4.17—Phase shift per section, θ, vs radian frequency ω for the conditions of Fig. 4.16.

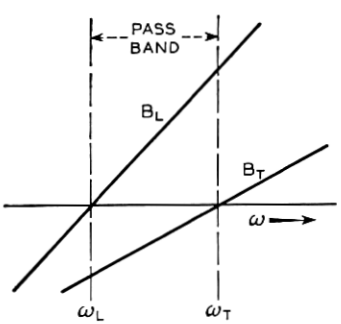

Fig. 4.18—Longitudinal and transverse susceptances which give $-\pi$ radians phase shift at the lower cutoff ($\omega = \omega_L$) and 0 degrees phase shift at the upper cutoff ($\omega = \omega_T$). This means a negative phase velocity.

It is of course possible to make $\omega_L > \omega_T$. In this case the situation is as shown in Fig. 4.18, the pass band extending from ω_L to ω_T. At $\omega = \omega_L$, $\cos \theta = -1$, $\theta = -\pi$. At $\omega = \omega_T$, $\cos \theta = 1$ and $\theta = 0$. In Fig. 4.19, assuming (4.46) and (4.47), θ has been plotted vs ω for $C_L/C_T = 1, 3, 10$.

The curves of Figs. 4.17 and 4.18 are not exact for any physical structure of the type shown in Fig. 4.10. In lumped circuit terms, they neglect coupling

between slots. They will be most accurate for structures with slots longitudinally far apart compared with the transverse dimensions, and least accurate for structures with slots close together. They do, however, form a valuable guide in understanding the performance of such structures and in evaluating the effect of the ratio of energies stored in the fields at the two cutoff frequencies.

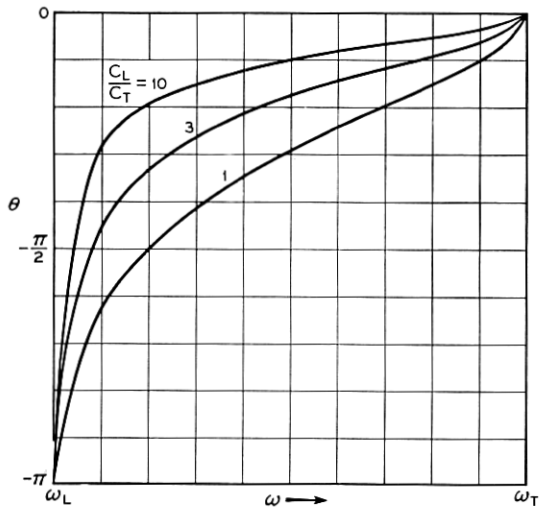

Fig. 4.19—Phase shift per section, θ, vs radian frequency, ω, for the conditions of Fig 4.18.

It is most likely that the voltages across the slots would be of most interest in connection with the circuit shown in Fig. 4.10. We can rewrite (4.41) in terms of B_T and B_L

$$V^2/P = \frac{1}{2(1 - 4B_L/B_T)(-B_T B_L)^{1/2}} \tag{4.49}$$

We see that V^2/P goes to 0 at $B_T = 0$ ($\omega = \omega_T$) and to infinity at $B_L = 0$ ($\omega = \omega_L$). In Fig. 4.20 assuming (4.46) and (4.47), $(V^2/P)(\omega_L C_L \omega_T C_T)$ is plotted vs ω for $C_L/C_T = 1, 3, 10$.

Let us consider another circuit, that shown in Fig. 4.11. We see that this consists of a number of resonators coupled together inductively. We might draw the equivalent circuits of these resonators as shown in Fig. 4.21. Here L and C are the effective inductance and the effective capacitance of the resonators without irises. They are chosen so that the resonant frequency ω_0 is given by

$$\omega_0 = \sqrt{LC} \tag{4.50}$$

and the variation of gap susceptance B with frequency is

$$\partial B/\partial\omega = 2C \tag{4.51}$$

The arrows show directions of current flow when the currents in the gap capacitances are all the same.

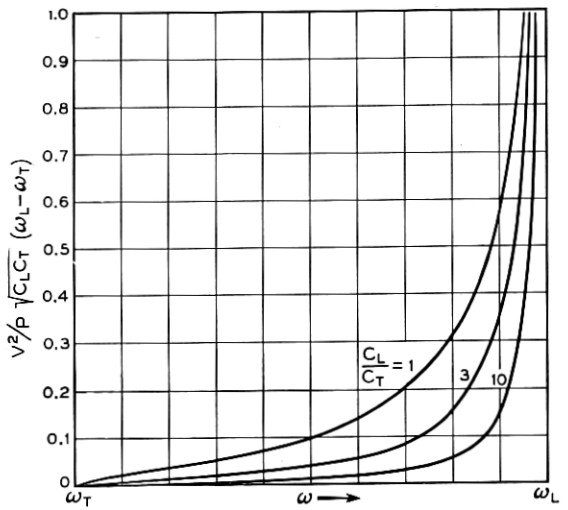

Fig. 4.20—A quantity proportional to $(E^2/\beta^2 P)$ vs ω for the conditions of Figs. 4.16 and 4.17.

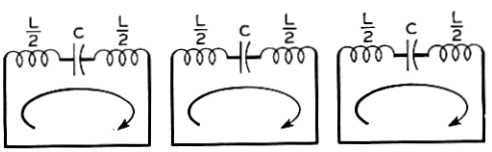

Fig. 4.21—A representation of the resonators of Fig. 4.11.

We can now represent the circuit of Fig. 4.11 by interconnecting the circuits of Fig. 4.21 by means of inductances L_M of Fig. 4.22. This gives a suitable representation, but one which is open to a minor objection: the gap capacitance does not appear across either a shunt or a series arm.

It is important to notice that there is another equally good representation, and there are probably many more. Suppose we draw the resonators as shown in Fig. 4.23 instead of as in Fig. 4.21. The inductance L and capacitance C are still properly given by 4.50 and 4.51. We can now interconnect the resonators inductively as shown in Fig. 4.24.

We should note one thing. In Fig. 4.21, the currents which are to flow in the common inductances of Fig. 4.22 flow in opposite directions when the

gap currents are in the same directions. In the representation of Fig. 4.23 the currents which will flow in the common inductances of Fig. 4.24 have been drawn in opposite directions, and we see that the currents in the gap capacitances flow alternately up and down. In other words, in Fig. 4.24, every other gap appears inverted. This can be taken into account by adding a phase angle $-\pi$ to θ as computed from (4.48).

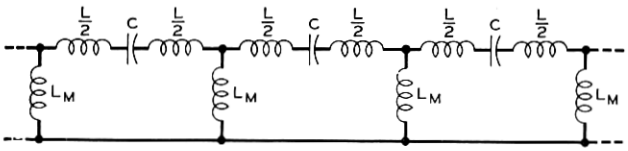

Fig. 4.22—The resonators of Fig. 4.11 coupled inductively.

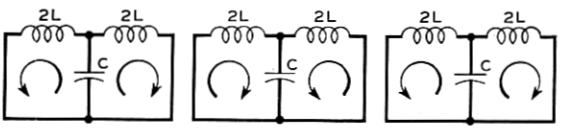

Fig. 4.23—Another representation of the resonators of Fig. 4.11.

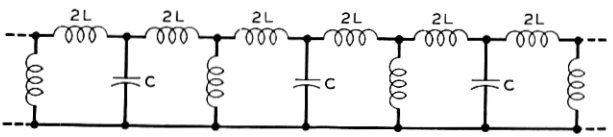

Fig. 4.24—Figure 4.23 with inductive coupling added.

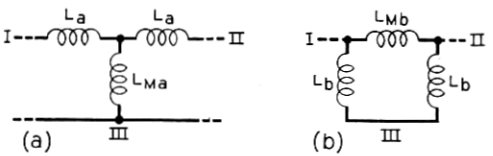

Fig. 4.25—A $T - \pi$ transformation used in connection with the circuit of Fig. 4.24.

Now, the T configuration of inductances in a of Fig. 4.25 can be replaced by the π configuration, b of Fig. 4.25. Imagine I and II to be connected together and a voltage to be applied between them and III. We see that

$$L_b = L_a + 2L_{Ma} \tag{4.52}$$

Imagine a voltage to be applied between I and II. We see that

$$1/L_a = 1/L_b + 2/L_{Mb} \tag{4.53}$$

If $L_{Ma} \ll L_a$, then L_b will be nearly equal to L_a and $L_{Mb} \gg L_b$.

By means of such a $T - \pi$ transformation we can redraw the equivalent circuit of Fig. 4.24 as shown in Fig. 4.26. The series susceptance B_1 is now

that of L_1, and the shunt susceptance is now that of the shunt resonant circuit consisting of C_2 (the effective capacitance of the resonators) and L_2.

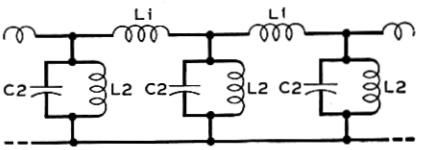

Fig. 4.26—The final representation of the circuit of Fig. 4.11.

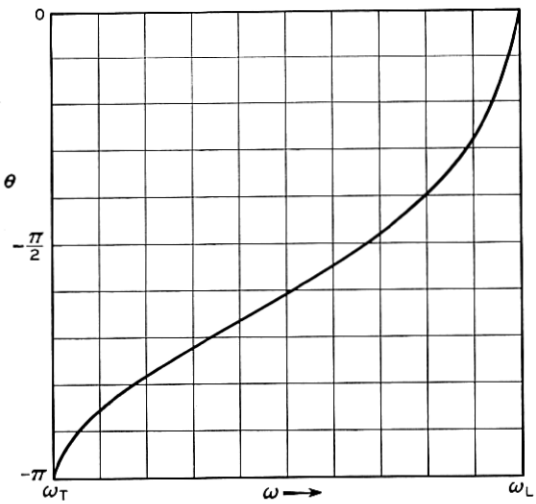

Fig. 4.27—The phase characteristic of the circuit of Fig. 4.11.

The transverse resonance, $B_2 = 0$, occurs at a frequency

$$\omega_T = \sqrt{C_2 L_2} \tag{4.54}$$

Near this frequency the transverse susceptance is given by

$$B_T = 2C_2(\omega - \omega_T) \tag{4.55}$$

The longitudinal resonance occurs at a frequency

$$\omega_L = \sqrt{2C_2 L_1 L_2/(L_1 + 2L_2)} \tag{4.56}$$

and near ω_L,

$$B_L = C_2(\omega - \omega_L) \tag{4.57}$$

These are just the forms we found in connection with the structure of Fig. 4.10; but we see that, in the case of the circuit of Fig. 4.11, the effective transverse capacitance is always twice the effective longitudinal capacitance ($C_L/C_T = 1/2$ in Fig. 4.19), and that $\omega_L > \omega_T$ for attainable volume of L_1.

We obtain θ vs ω by adding $-\pi$ to the phase angle from 4.48, using (4.55) and (4.57) in obtaining B_T and B_L. The phase angle vs. frequency is shown in Fig. 4.27. As the irises are made larger, the bandwidth, $\omega_L - \omega_T$, becomes larger, largely by a decrease in ω_L.

The voltage of interest is that across C_2, that is, that across the gap. From (4.37), (4.44), (4.45), (4.55) and (4.57) we obtain

$$V^2/P = 2/(-B_T B_L)^{1/2} \tag{4.58}$$

$$V^2/P = (\sqrt{2}/C_2)((\omega_L - \omega)(\omega - \omega_T))^{-1/2} \tag{4.59}$$

This goes to infinity at both $\omega = \omega_L$ and $\omega = \omega_T$. In Fig. 4.28, $(V^2/P)C_2\sqrt{\omega_L \omega_T}$ is plotted vs ω. This curve represents the performance of all narrow band structures of the type shown in Fig. 4.11.

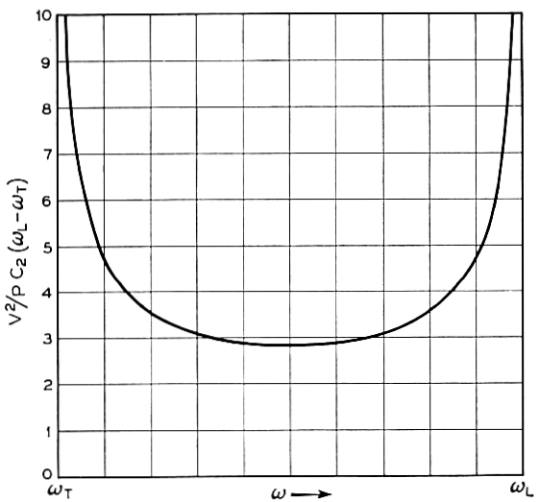

Fig. 4.28—A quantity proportional to $(E^2/\beta^2 P)$ for the circuit of Fig. 4.11, plotted vs radian frequency ω.

In a structure such as that shown in Fig. 4.11, there is little coupling between sections which are not adjacent, and hence the lumped-circuit representation used is probably quite accurate, and is certainly more accurate than in structures such as that shown in Fig. 4.10.

Other structures could be analyzed, but it is believed that the examples given above adequately illustrate the general procedures which can be employed.

4.4 Traveling Field Components

Filter-type circuits produce fields which are certainly not sinusoidal with distance. Indeed, with a structure such as that shown in Fig. 4.11, the elec-

trons are acted upon only when they are very near to the gaps. It is possible to analyze the performance of traveling-wave tubes on this basis[5]. The chief conclusion of such an analysis is that highly accurate results can be obtained by expressing the field as a sum of traveling waves and taking into account only the wave which has a phase velocity near to the electron velocity. Of course this is satisfactory only if the velocities of the other components are quite different from the electron velocity (that is, different by a fraction several times the gain parameter C).

As an example, consider a traveling-wave tube in which the electron stream passes through tubular sections of radius a, as shown in Fig. 4.29, and is acted upon by voltages appearing across gaps of length ℓ spaced L apart.

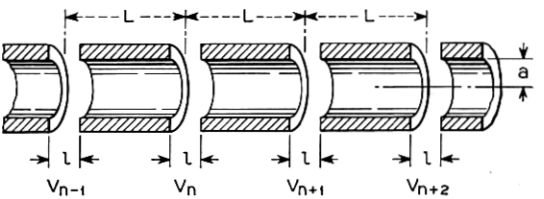

Fig. 4.29—A series of gaps in a tube of inside radius a. The gaps are ℓ long and are spaced L apart. Voltages V_n, etc., act across them.

A wave travels in some sort of structure and produces voltages across the gaps such that that across the nth gap, V, is

$$V_n = V_0 e^{-jn\theta} \tag{4.60}$$

where n is any integer.

We analyze this field into traveling-wave components which vary with distance as $\exp(-j\beta_m z)$ where

$$\beta_m = (\theta + 2m\pi)/L \tag{4.61}$$

where m is any positive or negative integer. Thus, the total field will be

$$E = \sum_{m=-\infty}^{\infty} E_m = \sum_{m=-\infty}^{\infty} A_m e^{-j\beta_m z} I_0(\gamma_m r) \tag{4.62}$$

$$\gamma_m^2 = \beta_m^2 - \beta_0^2 \tag{4.63}$$

Here $I_0(\gamma_m r)$ is a modified Bessel function, and γ_m has been chosen so that (4.62) satisfies Maxwell's equations.

[5] J. R. Pierce and Nelson Wax, "A Note on Filter-Type Traveling-Wave Amplifiers," *Proc. I.R.E.*, Vol. 37, pp. 622–625, June, 1949.

We will evaluate the coefficients by the usual means of Fourier analysis. Suppose we let $z = 0$ at the center of one of the gaps. We see that

$$\begin{aligned}\int_{-L/2}^{L/2} EE^* \, dz &= \sum_{m=-\infty}^{\infty} \int_{-L/2}^{L/2} A_m A_m^* I_0^2(\gamma_m r) \, dz \\ &= \sum_{m=-\infty}^{\infty} A_m A_m^* I_0^2(\gamma_m r) L\end{aligned} \tag{4.64}$$

All of the terms of the form $E_m E_p$, $p \neq m$ integrate to zero because the integral contains a term $\exp(-j2\pi(p - m)/L)z$.

Let us consider the field at the radius r. This is zero along the surface of the tube. We will assume with fair accuracy that it is constant and has a value $-V/\ell$ across the gap. Thus we have also at $r = a$,

$$\begin{aligned}\int_{-L/2}^{L/2} EE^* \, dz &= -(V/\ell) \sum_{m=-\infty}^{\infty} \int_{-\ell/2}^{\ell/2} A_m^* e^{-j\beta_m z} I_0(\gamma_m a) \, dz \\ &= -(V/\ell) \sum_{m=-\infty}^{\infty} (A_m^*) I_0(\gamma_m a) \left(\frac{e^{-j\beta_m \ell/2} - e^{j\beta_m \ell/2}}{j\beta} \right)\end{aligned} \tag{4.65}$$

We can rewrite this

$$\int_{-L/2}^{L/2} EE^* \, dz = -(V/\ell) \sum_{m=-\infty}^{\infty} A_m^* I_0(\gamma_m a) \frac{\sin(\beta_m \ell/2)}{(\beta_m \ell/2)} \tag{4.66}$$

By comparison with (4.64) we see that

$$A_m = -(V/L)(\sin(\beta_m \ell/2)/(\beta_m \ell/2))(1/I_0(\gamma a)) \tag{4.67}$$

This is the magnitude of the mth field component on the axis. The magnitude of the field at a radius r would be $I_0(\gamma r)$ times this.

The quantity $\beta_m \ell$ is an angle which we will call θ_g, the gap angle. Usually we are concerned with only a single field component, and hence can merely write γ instead of γ_m. Thus, we say that the magnitude E of the travelling field produced by a voltage V acting at intervals L is

$$E = -M(V/L) \tag{4.68}$$

$$M = \frac{\sin(\theta g/2)}{(\theta g/2)} \frac{I_0(\gamma r)}{I_0(\gamma a)} \tag{4.69}$$

$$\theta g = \beta \ell \tag{4.70}$$

The factor M is called the gap factor or the modulation coefficient*. For slow waves, γ is very nearly equal to β, and we can replace γr and γa by βr and βa. For unattenuated waves, M is a real positive number; and,

* This factor is often designated by β, but we have used β otherwise.

for the slowly varying waves with which we deal, we will always consider M as a real number.

The gap factor for some other physical arrangements is of interest. At a distance y above the two-dimensional array of strip electrodes shown in Fig. 4.30

$$M = \frac{\sin(\theta g/2)}{(\theta g/2)} e^{-\gamma y} \tag{4.71}$$

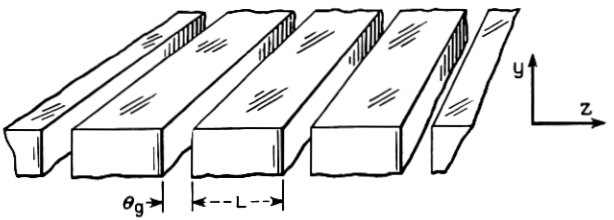

Fig. 4.30—A series of slots θ_g radians long separated by walls L long.

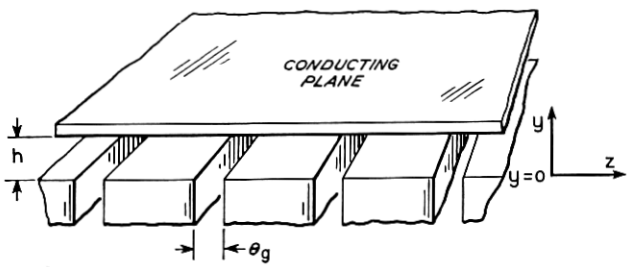

Fig. 4.31—A system similar to that of Fig. 4.30 but with the addition of an opposed conducting plane.

If we add a conducting plane a at $y = h$, as in Fig. 4.31,

$$M = \frac{\sin(\theta g/2)}{(\theta g/2)} \frac{\sinh \gamma(h - y)}{\sinh \gamma h} \tag{4.72}$$

For a symmetrical two-dimensional array, as shown in Fig. 4.32, with a separation of 2 h in the y direction and the fields above equal to the fields below

$$M = \frac{\sin(\theta g/2)}{(\theta g/2)} \frac{\cosh \gamma y}{\cosh \gamma h} \tag{4.73}$$

4.5 Effective Field and Effective Current

In Section 4.4 we have expressed a field component or "effective field" in terms of circuit voltage by means of a gap-factor or modulation coeffi-

cient M. This enables us to make calculations in terms of fields and currents at the electron stream.

The gap factor can be used in another way. A voltage appears across a gap, and the electron stream induces a current at the gap. At the electron stream the power P_1, produced in a distance L by a convection current i with the same z-variation as the field component considered, acting on the field component is

$$\begin{aligned} P_1 &= -Ei^*L \\ &= +(MV)i^* \end{aligned} \tag{4.74}$$

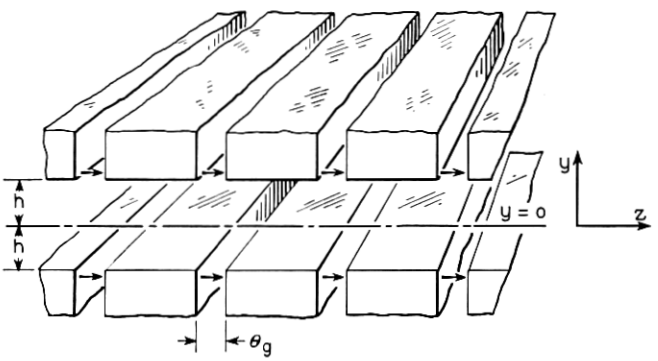

Fig. 4.32—A system of two opposed sets of slots.

At the circuit we observe some impressed current I flowing against the voltage V to produce a power

$$P_2 = VI^* \tag{4.75}$$

By the conservation of energy, these two powers must be the same, and we deduce that

$$I^* = Mi^* \tag{4.76}$$

or, since we take M as a real number

$$I = Mi \tag{4.77}$$

Thus, we have our choice of making calculations in terms of the beam current and a field component or effective field, or in terms of circuit voltage and an effective current, and in either case we make use of the modulation coefficient M.

Our gain parameter C^3 will be

$$C^3 = (V/L)^2M^2I_0/8\beta^2V_0$$

where V is circuit voltage. We can regard this in two ways. We can think of $-(V/L)M$ as the effective field at the location of the current I_0, or we can think of $M^2 I_0$ as the effective current referred to the circuit.

If we have a broad beam of electrons and a constant current density J_0 we compute (essentially as in Chapter III) a value of C^3 by integrating

$$C^3 = (1/8\beta^2 V_0) J_0 (V/L)^2 \int M^2 \, d\sigma \tag{4.78}$$

where $d\sigma$ is an element of area. We can think of the result in terms of an effective field E_e

$$E_e^2 = (V/L)^2 \frac{\int M^2 \, d\sigma}{\sigma} \tag{4.79}$$

where σ is the total beam area, and a total current σJ_0, or we can think of the integral (4.77) in terms of an effective current I_0 given by

$$I_0 = J_0 \int M^2 \, d\sigma \tag{4.80}$$

and the voltage at the circuit.

Of course, these same considerations apply to distributed circuits. Sometimes it is most convenient to think in terms of the total current and an effective field (as we did in connection with helices in Chapter III) and sometimes it is most convenient to think of the field at the circuit and an effective current. Either concept refers to the same mathematics.

4.6 Harmonic Operation

Of the field components making up E in (4.62) it is customary to regard the $m = 0$ component, for which $\beta = \theta/L$, as the *fundamental* field component, and the other components as *harmonic* components. These are sometimes called *Hartree harmonics*. If the electron speed is so adjusted that the interaction is with the $m = 0$ or fundamental component we have fundamental operation; if the electron speed is adjusted so that we have interaction with a harmonic component, we have harmonic operation.

There are several reasons for using harmonic operation in connection with filter-type circuits. For one thing the fundamental component may appear to be traveling backwards. Thus, for circuits of the type shown in Fig. 4.11, we see from Fig. 4.27 that θ is always negative. Now, in terms of the velocity v

$$\beta = \omega/v = \theta/L \tag{4.81}$$

and if θ is negative, v must be negative. However, consider the $m = 1$ component

$$\beta = \omega/v = (2\pi + \theta)/L \tag{4.82}$$

We see that, for this component, v is positive.

The interaction of electrons with backward-traveling field components will be considered later. Here it will merely be said that, in order to avoid interaction with waves traveling in both directions, one must avoid having the electron speed lie near both the speed of a forward component and the speed of a backward component.

In order that the fundamental component be slow, θ must be large or L must be small. The largest value of θ is that near one edge of the band, where θ approaches π. Thus, the largest fundamental value of β is π/L, and to make

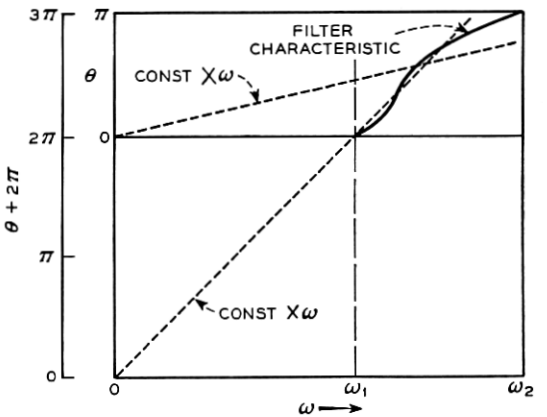

Fig. 4.33—The variation of phase with frequency for the fundamental (0 to π over the band) and a spatial harmonic (2π to 3π over the band). The dotted lines show ω divided by the electron velocity for the two cases. For amplification over a broad band the dotted curve should not depart much from the filter characteristic.

β large with $m = 0$ we must make L small and put the resonators very close together. This may be physically difficult or even impossible in tubes for very high frequencies. The alternative is to use a harmonic component, for which $\beta = (2m\pi + \theta)/L$.

Another reason for using harmonic operation is to achieve broad-band operation. The phase of a filter-type circuit changes by π radians between the lower cutoff frequency ω_1 and the upper cutoff frequency ω_2†. Now, for the wave velocity to be near to the electron velocity over a good part of the band, β must be nearly a constant times ω. Figure 4.33 shows how this can be approximately true for the $m = 1$ component even when it obviously won't be for the $m = 0$ or fundamental component. Similarly, for a filter with a narrower fractional bandwidth and hence a steeper curve of θ vs ω, a larger value of m might give a nearly constant value of v.

† The phase of some filters changes more than this, but they don't seem good candidates for traveling-wave tube circuits.

CHAPTER V

GENERAL CIRCUIT CONSIDERATIONS

Synopsis of Chapter

IN CHAPTERS III AND IV, helices and filter-type circuits have been considered. Other slow-wave circuits have been proposed, as, for instance, wave guides loaded continuously with dielectric material. One may ask what the best type of circuit is, or, indeed, in just what way do bad circuits differ from good circuits.

So far, we have as one criterion for a good circuit a high impedance, that is, a high value of $E^2/\beta^2 P$. If we want a broad-band amplifier we must have a constant phase velocity; that is, β must be proportional to frequency. Thus, two desirable circuit properties are: high impedance and constancy of phase velocity.

Now, $E^2/\beta^2 P$ can be written in the form

$$E^2/\beta^2 P = E^2/\beta^2 W v_g$$

where W is the stored energy per unit length for a field strength E, and v_g is the group velocity.

One way of making $E^2/\beta^2 P$ large is to make the stored energy for a given field strength small. In an electromagnetic wave, half of the stored energy is electric and half is magnetic. Thus, to make the total stored energy for a given field strength small we must make the energy stored in the electric field small. The energy stored in the electric field will be increased by the presence of material of a high dielectric constant, or by the presence of large opposed metallic surfaces, as in the circuits of Figs. 4.8 and 4.9. Thus, such circuits are poor as regards circuit impedance, however good they may be in other respects.

If the stored energy for a given field strength is held constant, $E^2/\beta^2 P$ may be increased by decreasing the group velocity. It is the phase velocity v which should match the electron speed. The group velocity v_g is given in terms of the phase velocity by (5.12). We see that the group velocity may be much smaller than the phase velocity if $-\partial v/\partial\omega$ is large. It is, for instance, a low group velocity near cutoff that accounts for the high impedance regions exhibited in Figs. 4.20 and 4.28. We remember, however, that, if the phase velocity of the circuit of a traveling-wave tube changes with frequency, the tube will have a narrow bandwidth, and thus the high

impedances attained through large values of $-\partial v/\partial\omega$ are useful over a narrow range of frequency only.

If we consider a broad electron stream of current density J_0, the highest effective value of E^2/β^2P, and hence the highest value of C, will be attained if there is current everywhere that there is electric field, and if all of the electric field is longitudinal. This leads to a limiting value of C, which is given by (5.23). There λ_0 is the free-space wavelength. The nearest practical approach to this condition is perhaps a helix of fine wire flooded inside and outside with electrons.

In many cases, it is desirable to consider circuits for use with a narrow beam of electrons, over which the field may be taken as constant. As the helix is a common as well as a very good circuit, it might seem desirable to use it as a standard for comparison. However, the group velocity of the helix differs a little from the phase velocity, and it seems desirable instead to use a sort of hypothetical circuit or field for which the stored energy is almost the same as in the helix, but for which the group velocity is the same as the phase velocity. This has been referred to in the text as a "forced sinusoidal field." In Fig. 5.3, $(E^2/\beta^2P)^{1/3}$ for the forced sinusoidal field is compared with $(E^2/\beta^2P)^{1/3}$ for the helix.

Several other circuits are compared with this: the circular resonators of Fig. 5.4 (the square resonators of Fig. 5.4 give nearly the same impedance) and the resonant quarter-wave and half-wave wires of Figs. 5.6 and 5.7. The comparison is made in Fig. 5.8 for three voltages, which fix three phase velocities. In each case it is assumed that in some way the group velocity has been made equal to the phase velocity. Thus, the comparison is made on the basis of stored energies. The field is taken as the field at radius a (corresponding to the surface of the helix) in the case of the forced sinusoidal field, and at the point of highest field in the case of the resonators.

We see from Figs. 5.8 and 5.3 that a helix of small radius is a very fine circuit.

In circuits made up of a series of resonators, the group velocity can be changed within wide limits by varying the coupling between resonators, as by putting inductive or capacitive irises between them. Thus, even circuits with a large stored energy can be made to have a high impedance by sacrificing bandwidth.

The circuits of Fig. 5.4 have a large stored energy because of the large opposed surfaces. The wires of Fig. 5.6 have a small stored energy associated entirely with "fringing fields" about the wires. The narrow strips of Fig. 5.5 have about as much stored energy between the opposed flat surfaces as that in the fringing field, and are about as good as the half-wave wires of Fig. 5.7.

An actual circuit made up of resonators such as those of Fig. 5.4 will be

worse than Fig. 5.8 implies. Thus, there is a decrease of $(E^2/\beta^2P)^{1/3}$ due to wall thickness. Thickening the flat opposed walls of the resonators decreases the spacing between the opposed surfaces, increases the capacitance and hence increases the stored energy for a given gap voltage. In Fig. 5.9 the factor f by which $(E^2/\beta^2P)^{1/3}$ is reduced is plotted vs. the ratio of the wall thickness t to the resonator spacing L.

There is a further reduction of effective field because of the electrical length, θ in radians, of the space between opposed resonator surfaces. The lower curve in Fig. 5.10 gives a factor by which $(E^2/\beta^2P)^{1/3}$ is reduced because of this. If the resonator spacing, θ_t in radians, is greater than 2.33 radians, it is best to make the opening, or space between the walls, only 2.33 radians long by making the opposed disks forming the walls very thick.

There is of course a further loss in effective field, both in the helix and in circuits made up of resonators, because of the falling-off of the field toward the center of the aperture through which the electrons pass. This was discussed in Chapter IV.

Finally, it should be pointed out that the fraction of the stored energy dissipated in losses during each cycle is inversely proportional to the Q of the circuit or of the resonators forming it. The distance the energy travels in a cycle is proportional to the group velocity. Thus, for a given Q the signal will decay more rapidly with distance if the group velocity is lowered (to increase E^2/β^2P). Equations (5.38), (5.42) and (5.44) pertain to attenuation expressed in terms of group velocity. The table at the end of the chapter shows that a circuit made up of resonators and having a low enough group velocity to give it an impedance comparable with that of a helix can have a very high attenuation.

5.1 Group and Phase Velocity

Suppose we use a broad video pulse $F(t)$, containing radian frequencies p lying in the range 0 to p_0, to modulate a radio-frequency signal of radian frequency ω which is much larger than p_0, so as to give a radio-frequency pulse $f(t)$

$$f(t) = e^{j\omega t}F(t) \tag{5.1}$$

the functions $F(t)$ and $f(t)$ are indicated in Fig. 5.1.

$F(t)$, which is a real function of time, can be expressed by means of its Fourier transform in terms of its frequency components

$$F(t) = \int_{p_0}^{p_0} A(p)e^{jpt}\,dp \tag{5.2}$$

Here $A(p)$ is a complex function of p, such that $A(-p)$ is the complex conjugate of $A(p)$ (this assures that $F(t)$ is real).

With $F(t)$ expressed as in (5.2), we can rewrite (5.1)

$$f(t) = \int_{-p_0}^{p_0} A(p)e^{j(\omega+p)t}\,dp \tag{5.3}$$

Now, suppose, as indicated in Fig. 5.2, we apply the *r-f* pulse $f(t)$ to the input of a transmission system of length L with a phase constant β which

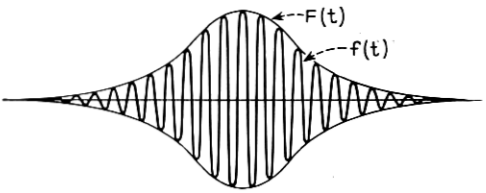

Fig. 5.1—A radio-frequency pulse varying with time as $f(t)$. The envelope varies with time as $F(t)$. The pulse might be produced by modulating a radio-frequency source with $F(t)$.

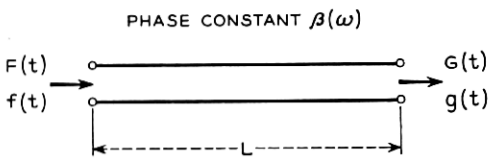

Fig. 5.2—When the pulse of Fig. 5.1 is applied to a transmission system of length L and phase constant $\beta(\omega)$ (a function of ω), the output pulse $g(t)$ has an envelope $G(t)$.

is a function of frequency. Let us assume that the system is lossless. The output $g(t)$ will then be

$$g(t) = \int_{-p_0}^{p_0} A(p)e^{j((\omega+p)t-\beta L)}\,dp \tag{5.4}$$

We have assumed that p_0 is much smaller than ω. Let us assume that over the range $\omega - p_0$ to $\omega + p_0$, β can be adequately represented by

$$\beta = \beta_0 + \frac{\partial\beta}{\partial\omega}\,p \tag{5.5}$$

In this case we obtain

$$g(t) = e^{j(\omega t-\beta_0 L)} \int_{-p_0}^{p_0} A(p)\, e^{jp(t-(\partial\beta/\partial\omega)L)}\,dp \tag{5.6}$$

The envelope at the output is

$$G(t) = \int_{-p_0}^{p_0} A(p)\, e^{jp(t-(\partial\beta/\partial\omega)L)}\,dp \tag{5.7}$$

By comparing this with (5.2) we see that

$$G(t) = F\left(t - \frac{\partial\beta}{\partial\omega} L\right) \tag{5.8}$$

In other words, the envelope at the output is of the same shape as at the input, but arrives a time τ later

$$\tau = \frac{\partial\beta}{\partial\omega} L \tag{5.9}$$

This implies that it travels with a velocity v_g

$$v_g = L/\tau = \left(\frac{\partial\beta}{\partial\omega}\right)^{-1} \tag{5.10}$$

This velocity is called the group velocity, because in a sense it is the velocity with which the group of frequency components making up the pulse travels down the circuit. It is certainly the velocity with which the energy stored in the electric and magnetic fields of the circuit travels; we could observe physically that, if at one time this energy is at a position x, a time t later it is at a position $x + v_g t$.

If the attenuation of the transmission circuit varies with frequency, the pulse shape will become distorted as the pulse travels and the group velocity loses its clear meaning. It is unlikely, however, that we shall go far wrong in using the concept of group velocity in connection with actual circuits.

We have used earlier the concept of phase velocity, which we have designated simply as v. In terms of phase velocity,

$$\beta = \frac{\omega}{v} \tag{5.11}$$

We see from (5.10) that in terms of phase velocity v the group velocity v_g is

$$v_g = v\left(1 - \frac{\omega}{v}\frac{\partial v}{\partial\omega}\right)^{-1} \tag{5.12}$$

For interaction of electrons with a wave to give gain in a traveling-wave tube, the electrons must have a velocity near the phase velocity v. Hence, for gain over a broad band of frequencies, v must not change with frequency; and if v does not change with frequency, then, from (5.12), $v_g = v$.

We note that the various harmonic components in a filter-type circuit have different phase velocities, some positive and some negative. The group

velocity is of course the same for all components, as they are all aspects of one wave. Relation (4.61) is consistent with this:

$$\beta_m = (\theta + 2m\pi)/L \tag{4.61}$$

$$1/v_g = \partial\beta_m/\partial\omega = (\partial\theta/\partial\omega)/L \tag{5.13}$$

5.2 Gain and Bandwidth in a Traveling-Wave Tube

We can rewrite the impedance parameter E^2/β^2P in terms of stored energy per unit length W for a field strength E, and a group velocity v_g. If W is the stored energy per unit length, the power flow P is

$$P = Wv_g \tag{5.14}$$

and, accordingly, we have

$$E^2/\beta^2P = E^2/\beta^2Wv_g \tag{5.15}$$

And, for the gain parameter, we will have

$$C = (E^2/\beta^2Wv_g)^{1/3}(I_0/8V_0)^{1/3} \tag{5.16}$$

For example, we see from Fig. 4.20 that E^2/β^2P for the circuit of Fig. 4.10 goes to infinity at the upper cut-off. From Fig. 4.17 we see that $\partial\theta/\partial\omega$, and hence $1/v_g$, go to infinity at the upper cutoff, accounting for the infinite impedance. We see also that $\partial\theta/\partial\omega$ goes to infinity at the lower cutoff, but there the slot voltage and hence the longitudinal field also go to zero and hence E^2/β^2P does not go to infinity but to zero instead.

In the case of the circuit of Fig. 4.11, the gap voltage and hence the longitudinal field are finite for unit stored energy at both cutoffs. As $\partial\theta/\partial\omega$ is infinite at both cutoffs, V^2/P and hence E^2/β^2P go to infinity at both cutoffs, as shown in Fig. 4.28.

To get high gain in a traveling-wave tube at a given frequency and voltage (the phase velocity is specified by voltage) we see from (5.16) that we must have either a small stored energy per unit length for unit longitudinal field, or a small group velocity, v_g.

To have amplification over a broad band of frequencies we must have the phase velocity v substantially equal to the electron velocity over a broad band of frequencies. This means that for very broad-band operation, v must be substantially constant and hence in a broad-band tube the group velocity will be substantially the same as the phase velocity.

If the group velocity is made smaller, so that the gain is Increased, the range of frequencies over which the phase velocity is near to the electron velocity is necessarily decreased. Thus, for a given phase velocity, as the group velocity is made less the gain increases but the bandwidth decreases.

Particular circuits can be compared on the basis of (E^2/β^2P) and band-

width. We have discussed the impedance and phase or velocity curves in Chapters III and IV. Field[1] has compared a coiled waveguide structure with a series of apertured disks of comparable dimensions. Both of these structures must have about the same stored energy for a given field strength. He found the coiled waveguide to have a low gain and broad bandwidth as compared with the apertured disks. We explain this by saying that the particular coiled waveguide he considered had a higher group velocity than did the apertured disk structure. Further, if the coiled waveguide could be altered in some way so as to have the same group velocity as the apertured disk structure it would necessarily have substantially the same gain and bandwidth.

In another instance, Mr. O. J. Zobel of these Laboratories evaluated the effect of broad-banding a filter-type circuit for a traveling-wave tube by m-derivation. He found the same gain for any combination of m and bandwidth which made $v = v_g(\partial v/\partial\omega = 0)$. We see this is just a particular instance of a general rule. The same thing holds for any type of broad-banding, as, by harmonic operation.

5.3 A Comparison of Circuits

The group velocity, the phase velocity and the ratio of the two are parameters which are often easily controlled, as, by varying the coupling between resonators in a filter composed of a series of resonators. Moreover, these parameters can often be controlled without much affecting the stored energy per unit length. For instance, in a series of resonators coupled by loops or irises, such as the circuit of Fig. 4.11, the stored energy is not much affected by the loops or irises unless these are very large, but the phase and group velocities are greatly changed by small changes in coupling.

Let us, then, think of circuits in terms of stored energy, and regard the phase and group velocities and their ratio as adjustable parameters. We find that, when we do this, there are not many essentially different configurations which promise to be of much use in traveling-wave tubes, and it is easy to make comparisons between extreme examples of these configurations.

5.3a Uniform Current Density throughout Field

Suppose we have a uniform current density J_0 wherever there is longitudinal electric field. We might approximate this case by flooding a helix of very fine wire with current inside and outside, or by passing current through a series of flat resonators whose walls were grids of fine wire.

[1] Lester M. Field, "Some Slow-Wave Structures for Traveling-Wave Tubes," *Proc. I.R.E.*, Vol. 37, pp. 34–40, January 1949.

In the latter case, if resonators had parallel walls of very fine mesh normal to the direction of electron motion there would be substantially no transverse electric field. All the electric field representing stored energy would act on the electron stream. In this case, we would have

$$W = \frac{\epsilon}{2} \int E^2 \, d\Sigma \tag{5.17}$$

Here $d\Sigma$ is an elementary area normal to the direction of propagation. W given by this expression is the total electric and magnetic stored energy per unit length. Where E is less than its peak value, the magnetic energy makes up the difference.

In evaluating $E^2 I_0$ in (5.16) we will have as an effective value

$$(EI_0)_{\text{eff}} = J_0 \int E \, d\Sigma \tag{5.18}$$

Hence, we will have for the gain parameter C

$$C = \left(\frac{J_0 \int E^2 \, d\Sigma}{\left(\frac{\omega}{v}\right)^2 \left(\frac{\epsilon}{2} \int E^2 \, d\Sigma\right) v_0 (8V_0)} \right)^{1/3}$$

$$C = \left(\frac{J_0}{4 \left(\frac{\omega}{v}\right)^2 \epsilon v_0 V_0} \right)^{1/3} \tag{5.19}$$

It is of interest to put this in a slightly different form. Suppose λ_0 is the free-space wavelength. Then

$$\frac{\omega}{v} = \frac{2\pi}{\lambda_0} \frac{c}{v} \tag{5.20}$$

where c is the velocity of light

$$c = 3 \times 10^{10} \text{ cm/sec} = 3 \times 10^8 \text{ m/sec}$$

Further, we have for synchronism between the electron velocity u_0 and the phase velocity v

$$v^2 = 2\eta V_0 \tag{5.21}$$

Also

$$c = 1/\sqrt{\mu\epsilon}$$

$$\epsilon = 1/c\sqrt{\mu/\epsilon} \tag{5.22}$$

$$\sqrt{\mu/\epsilon} = 377 \text{ ohms}$$

Using (5.20), (5.21), (5.22) in connection with (5.19), we obtain

$$C = \left(\frac{\eta\sqrt{\mu/\epsilon}\ J_0\lambda_0^2}{16\pi^2 c v_g}\right)^{1/3} = 11.16\ (J_0\lambda_0^2/v_g)^{1/3} \tag{5.23}$$

We have in (5.23) an expression for the gain parameter C in case longitudinal fields only are present and in case there is a uniform current density J_0 wherever there is a longitudinal field.

In a number of cases, as in case of a large-diameter helix, or of a resonator with large apertures, the stored energy due to the transverse field is about equal to that due to the longitudinal field and C will be $2^{-1/3}$ times as great as the value of C given by (5.23). Thus, the value of C given by (5.23), or even $2^{-1/3}$ times this, represents an unattainable ideal. It is nevertheless of interest in indicating how limiting behavior depends on various parameters. For instance, we see that if the wavelength λ_0 is made shorter, a higher current density must be used if C is not to be lowered; for a constant C the current density must be such as to give a constant current through a square a wavelength on a side.

In the table below, some values of C have been computed from (5.23) for various wavelengths and current densities. The broad-band condition of equal phase and group velocities has been assumed, and the voltage has been taken as 1,000 volts.

Wavelength Cm \ Amp/cm²	.1	1
5	.060	.130
.5	.013	.028

For larger voltages, C will be smaller. C can of course be made larger by making the group velocity smaller than the phase velocity.

Of course, if the electron stream does not pass through some portions of the field, C will be smaller than given by (5.23). C will also be less if there are "harmonic" field components which do not vary in the z direction as $\exp(j\omega z/v)$.

5.3b Narrow Beams

Usually, no attempt is made to fill the entire field with electron flow even though this is necessary in getting a large value of C for a given current density. Instead a narrow electron beam is shot through a region of high

field. We then wish to relate the peak field strength to the stored energy in comparing various circuits.

Let us first consider a helically conducting sheet of radius a. The upper curve of Fig. 5.3 shows $(E^2/\beta^2 P)^{1/3}(v/c)^{1/3}$ vs. βa. In obtaining this curve it was assumed that $v \ll c$, so that γ can be taken as equal to β. The field E is the longitudinal field at the surface of the helically conducting cylinder. Figure 5.3 can be obtained from Fig. 3.4 by multiplying $F(\gamma a)$ by $(I_0(\gamma a))^{2/3}$ to give a curve valid for the field at $r = a$.

The helix has a very small circumferential electric field which represents "useless" stored energy. The lower curve of Fig. 5.3 is based on the stored electric energy of an axially symmetrical sinusoidal field impressed at the radius a.† This field has no circumferential component but is otherwise the

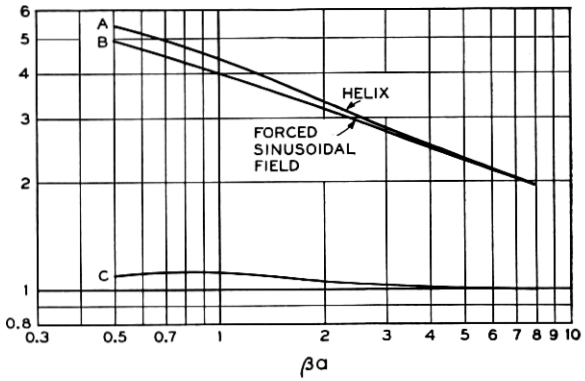

Fig. 5.3—The impedance parameter $(E^2/\beta^2 P)^{1/3}$ compared for a helically conducting sheet (A) and a forced sinusoidal field (B) with a group velocity equal to the phase velocity. The helix has a higher impedance because the phase velocity is higher than the group velocity by a radio shown to the $\frac{1}{3}$ power by curve C.

same as the electric field of the helix (again assuming $v \ll c$). We can imagine such a field propagating because of an inductive sheet at the radius a, which provides stored magnetic energy enough to make the electric and magnetic energies equal. The quantity plotted vs. βa is $(E^2/\beta^2 P)^{1/3}$ $(v/c)^{1/3}$ $(v_g/v)^{1/3}$.

The forced sinusoidal field is not the field of some particular circuit for which a certain group velocity v_g corresponds to a given phase velocity v. Hence, the factor $(v_g/v)^{1/3}$ is included in the ordinate, so that the curve will be the same no matter what group velocity is assumed. For the helically conducting sheet, a definite group velocity goes with a given phase velocity. In Fig. 5.3, the ordinate of the curve for the helically conducting sheet does not contain the factor $(v_g/v)^{1/3}$. If, for instance, we assume $v_g = v$

† See Appendix III.

in connection with the curve for the forced sinusoidal field, then the two ordinates are both $(E^2/\beta^2P)^{1/3}$ $(v/c)^{1/3}$ and the curve for the sheet is higher than that for the forced field because, for the helically conducting sheet,

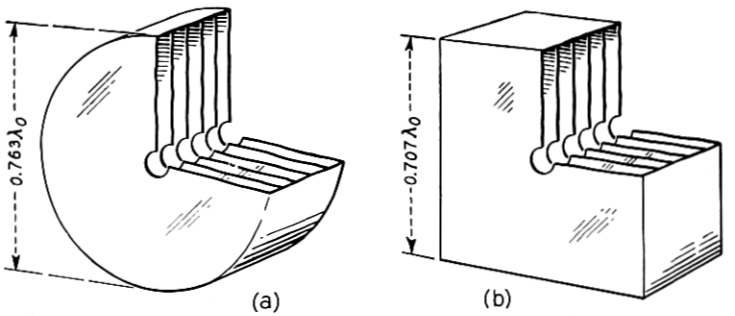

Fig. 5.4—Pillbox and rectangular resonators. When a number of resonators are coupled one to the next, a filter-type circuit is formed.

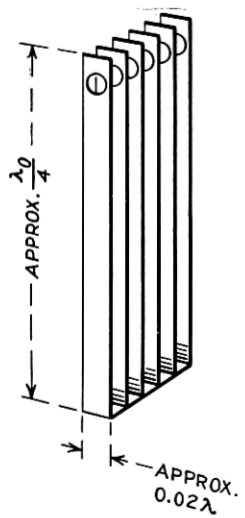

Fig. 5.5—Resonators with the opposing parallel surfaces reduced to lower stored energy and increase impedance.

$v_g < v$ for small values of γa. Curve C shows $(v/v_g)^{1/3}$ for the sheet vs. βa. Aside from the influence of group velocity, we might have expected the curve for the sheet to be a little lower than that for the forced field because of the energy associated with the transverse electric field component of the sheet. This, however, becomes small in comparison with the transverse magnetic component when $v \ll c$, as we have assumed.

Various other circuits will be compared, using the impressed sinusoidal field as a sort of standard of reference.

One of the circuits which will be considered is a series of flat resonators coupled together to make a filter. Figure 5.4a shows a series of very thin pillboxes with walls of negligible thickness. A small central hole is provided for the electron stream, and the field E is to be measured at the edge of this hole. The diameter is chosen to obtain resonance at a wavelength λ_0. Figure 5.4b shows a similar series of flat square resonators.

For the round resonators it is found that*

$$(E^2/\beta^2P)^{1/3} = 5.36\ (v/c)^{1/3}\ (v/v_g)^{1/3} \tag{5.24}$$

for the square resonators*

$$(E^2/\beta^2P)^{1/3} = 5.33\ (v/c)^{1/3}\ (v/v_g)^{1/3} \tag{5.25}$$

For practical purposes these are negligibly different.

* See Appendix III.

Suppose we wanted to improve on such circuits by reducing the stored energy. An obvious procedure would be to cut away most of the flat opposed surfaces as shown in Fig. 5.5. This reduces the energy stored between the resonator walls, but results in energy storage outside of the open edges, energy associated with a "fringing field."

Going to an extreme, we might consider an array of closely spaced very fine wires, as shown in Fig. 5.6. Here there are no opposed flat surfaces, and all of the electric field is a fringing field; we have reached an irreducible minimum of stored energy in paring down the resonator.

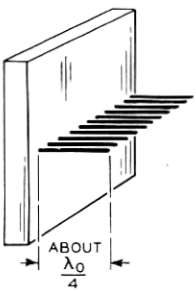

Fig. 5.6—Quarter-wave wires, which have a minimum of stored energy.

The structure of Fig. 5.6 has not been analyzed exactly, but that of Fig. 5.7 has. In Fig. 5.7, we have an array of fine, closely spaced half-wave wires between parallel planes.* This should have roughly twice the stored energy of Fig. 5.6, and we will estimate $(E^2/\beta^2 P)^{1/3}$ for Fig. 5.6 on this basis. We obtain in Appendix III:

For the half-wave wires,

$$(E^2/\beta^2 P)^{1/3} = 6.20\ (v/v_g)^{1/3} \qquad (5.25)$$

and hence for the quarter-wave wires, approximately

$$(E^2/\beta^2 P)^{1/3} = 7.81\ (v/v_g)^{1/3} \qquad (5.26)$$

As we have noted, (v/c), which appears in the expression for $(E^2/\beta^2 P)^{1/3}$ for the sinusoidal field impressed at radius a and in (5.24) and (5.25), is a

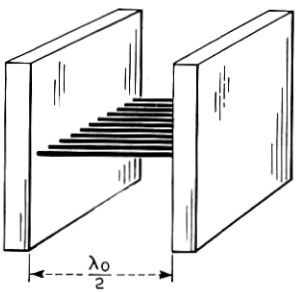

Fig. 5.7—Half-wave wires between parallel planes. The stored energy can be calculated for this configuration, assuming the wires to be very fine. The circuit does not propagate a wave unless added coupling is provided.

function of the accelerating voltage. Figure 5.8 makes a comparison between the sinusoidal field impressed at a radius a, curve A; the flat resonators, either circular or square, B; the half-wave wires, C; and the quarter-

* There is no transverse magnetic wave propagation along such a circuit unless extra coupling or loading is provided. Behavior of nonpropagating circuits in the presence of an electron stream is considered in Section 4 of Chapter XIV.

wave wires C'. In all cases, it is assumed that the coupling is so adjusted as to make $(v_g/v) = 1$ (broad-band condition).

What sort of information can we get from the curves of Fig. 5.8? Consider the curves for 1,000 volts. Suppose we want to cut down the opposed areas of resonators, as indicated in Fig. 5.5, so as to make them as good as half-wave wires (curve C). The edge capacitance in Fig. 5.5 will be about equal to that for quarter-wave wires (curve C'). Curve C' is about 3.7 times as high as curve B, and hence represents only about $(1/3.7)^3 = .02$ as much capacitance. If we make the opposed area in Fig. 5.5 about .01 that in Fig. 5.4a or b, the capacitance* between opposed surfaces will equal the edge

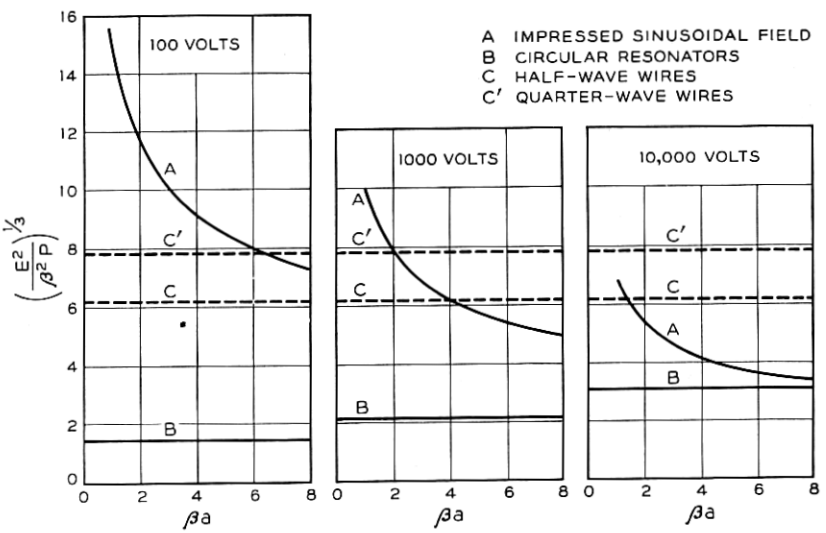

Fig. 5.8—Comparisons in terms of impedance parameter of an impressed sinusoidal field (A), circular resonators (B), half-wave wires (C) and quarter-wave wires (C') assuming the group and phase velocities to equal the electron velocity. The radius of the impressed sinusoidal field is a.

capacitance and the total stored energy will be twice that for quarter-wave wires, or equal to that for half-wave wires. This area is shown approximately to scale relative to Fig. 5.4 in Fig. 5.5. Thus, at 1,000 volts the resonant strips of Fig. 5.5 are about as good as fine, closely spaced half-wave wires.

Suppose again that we wish at 1,000 volts to make the gain of the resonators of Fig. 5.4 (or of a coiled waveguide) as good as that for a helix with $\beta a = 3$. For $\beta a = 3$ the helix curve A is about 3.2 times as high as the resona-

* This takes into account a difference in field distribution—that in Fig. 5.4b.

tor curve B. As $(E^2/\beta^2 P)^{1/3}$ varies as $(v/v_g)^{1/3}$, we must adjust the coupling between resonators so as to make

$$v_g = v/(3.2)^3 = .031\ v$$

in order to make $(E^2/\beta^2 P)^{1/3}$ the same for the resonators as for the helix. From (5.12) we see that this means that a change in frequency by a fraction .002 must change v by a fraction .06. Ordinarily, a fractional variation of v of $\pm .03$ would cause a very serious falling off in gain. At 3,000 mc the total frequency variation of .002 times in v would be 6 mc. This is then a measure of the bandwidth of a series of resonators used in place of a helix for which $\beta a = 3$ and adjusted to give the same gain.

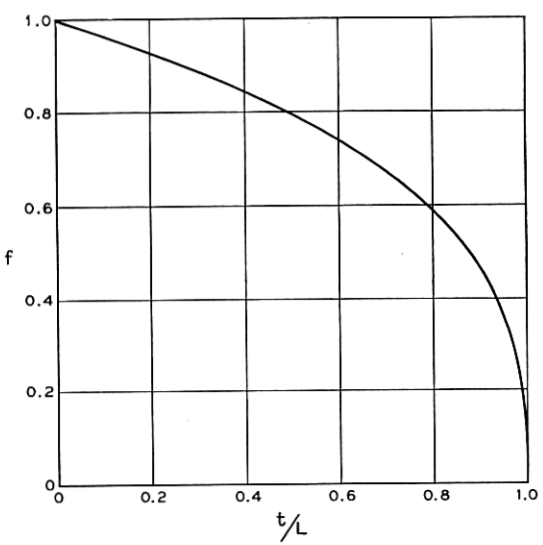

Fig. 5.9—The factor f by which $(E^2/\beta^2 P)^{1/3}$ for a series of resonators such as those of Fig. 5.4 is reduced because of wall thickness t, in relation to gap spacing L.

5.4 Physical Limitations

In Section 3.3b the resonators were assumed to be very thin and to have walls of zero thickness. Of course the walls must have finite thickness, and it is impractical to make the resonators extremely thin. The wall thickness and the finite transit time across the resonators both reduce $E^2/\beta^2 P$.

5.4a Effect of Wall Thickness

Consider the resonators of Fig. 5.4. Let L be the spacing between resonators ($1/L$ resonators per unit length), and t be the wall thickness. Thus, the gap length is $(L - t)$. Suppose we keep L and the voltage across each

resonator constant, so as to keep the field constant, but vary t. The capacitance will be proportional to $(L - t)^{-1}$ and, as the stored energy is the voltage squared times the capacitance, we see that $(E^2/\beta^2 P)^{1/3}$ will be reduced by a factor f,

$$f = (1 - t/L)^{1/3} \tag{5.27}$$

The factor f is plotted vs. t/L in Fig. 5.9.

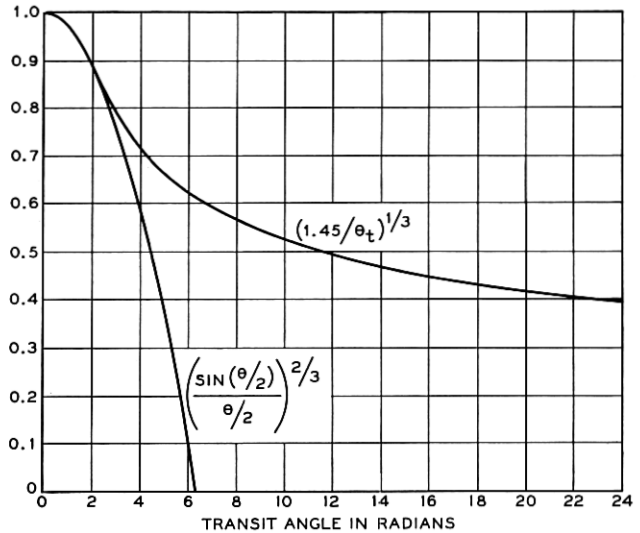

Fig. 5.10—The lower curve shows the factor by which $E^2/\beta^2 P$ is reduced by gap length, θ in radians. If the gap spacing is greater than 2.33 radians, it is best to make the gap 2.33 radians long. Then the upper curve applies.

5.4b Transit Time

As it is impractical to make the resonators infinitely thin, there will be some transit angle θ_g across the resonator, where

$$\theta_g = \beta \ell \tag{5.28}$$

Here ℓ is the space between resonator walls, or, the length of the gap. If we assume a uniform electric field between walls, the gap factor M, that is, the ratio of peak energy gained in electron volts to peak resonator voltage, or the ratio of the magnitude of the sinusoidal field component produced to that which would be produced by the same number of infinitely thin gaps with the same voltages, will be (from (4.69) with $r = a$)

$$M = \frac{\sin(\theta_g/2)}{\theta_g/2} \tag{5.29}$$

For a series of resonators θ_g long with infinitely thin walls $E^2/\beta^2 P$ will be less than the values given by (5.24) and (5.25) by a factor $M^{2/3}$. This is plotted vs. θ_g in Fig. 5.10.

5.4c Fixed Gap Spacing

Suppose it is decided in advance to put only one gap in a length specified by the transit angle θ_t. How wide should the gap be made, and how much will $E^2/\beta^2 P$ be reduced below the value for very thin resonators and infinitely thin walls?

Let us assume that all the stored energy is energy stored between parallel planes separated by the gap thickness, expressed in radians as θ or in distance as L

$$\theta_t = \beta \ell$$
$$\theta_g = \beta L$$

Here ℓ is the gap spacing and L is the spacing between resonators.

From Section 4.4 of Chapter IV we see that if V is the gap voltage, the field strength E is given by

$$E = MV/L$$

The stored energy per unit length, W, will be

$$W = W_0 V^2/\ell L \tag{5.30}$$

Here W_0 is a constant depending on the cross-section of the resonators. Thus, for unit field strength, the stored energy will be

$$\begin{aligned} W &= W_0 L/\ell M^2 \\ W &= W_0(\theta_t/\theta_g)(\theta_g/2)^2/\sin^2(\theta_g/2) \end{aligned} \tag{5.31}$$

We see that W_0 is merely the value of W when $\theta_t = \theta_g$ and $\theta_g = 0$, or, for zero wall thickness and very thin resonators. Thus, the ratio W/W_0 relates the actual stored energy per unit length per unit field to this optimum stored energy for resonators of the same cross section.

For $\theta_t < 2.33$, W/W_0 is smallest (best) for $\theta_g = \theta_t$ (zero wall thickness). For larger values of θ_t, the optimum value of θ_g is 2.33 radians and for this optimum value

$$(W_0/W)^{1/3} = (1.450/\theta_t)^{1/3} \tag{5.32}$$

If $\theta_t < 2.33$, it is thus best to make $\theta_g = \theta_t$. Then $(E^2/\beta^2 P)^{1/3}$ is reduced by the factor $[\sin(\theta/2)/(\theta/2)]^{2/3}$, which is plotted in Fig. 5.10. If $\theta_t > 2.33$, it is best to make $\theta = 2.33$. Then $(E^2/\beta^2 P)^{1/3}$ is reduced from the

value for thin resonators with infinitely thin walls by a factor given by (5.32), which is plotted vs. θ_t in Fig. 5.10.

If there are edge effects, the optimum gap spacing and the reduction in $(E^2/\beta^2 P)^{1/3}$ will be somewhat different. However, Fig. 5.10 should still be a useful guide.

In case of wide gap separation (large θ_t), there would be some gain in using reentrant resonators, as shown in Fig. 4.11, in order to reduce the capacitance. How good can such a structure be? Certainly, it will be worse than a helix. Consider merely the sections of metal tube with short gaps, which surround the electron beam. The shorter the gaps, the greater the capacitance. The space outside the beam has been capacitively loaded, which tends to reduce the impedance. This capacitance can be thought of as being associated with many spatial harmonics in the electric field, which do not contribute to interaction with the electrons.

5.5 Attenuation

Suppose we have a circuit made up of resonators with specified unloaded Q.† The energy lost per cycle is

$$W_L = 2\pi W_S/Q \tag{5.33}$$

In one cycle, however, a signal moves forward a distance L, where

$$L = v_g/f \tag{5.34}$$

The fractional energy loss per unit distance, which we will call 2α, is

$$2\alpha = \frac{W_L}{W_S}\frac{1}{L} \tag{5.35}$$

whence

$$\alpha = \frac{\omega}{2Qv_g} \tag{5.36}$$

So defined, α is the attenuation constant, and the amplitude will decay along the circuit as $\exp(-\alpha z)$.

The wavelength, λ, is given by

$$\lambda = v/f = 2\pi v/\omega \tag{5.37}$$

The loss per wavelength in db is

$$\text{db/wavelength} = 20 \log_{10} \exp(\alpha\lambda)$$

$$\text{db/wavelength} = \frac{27.3}{Q}\frac{v}{v_g} \tag{5.38}$$

† Disregarding coupling losses, the circuit and the resonantors will both have this same Q.

We see that, for given values of v and Q, decreasing the group velocity, which increases $E^2/\beta^2 P$, also increases the attenuation per wavelength.

5.5a Attenuation of Circuits

For various structures, Q can be evaluated in terms of surface resistivity, R, the intrinsic resistance of space, $\sqrt{\mu/\epsilon} = 377$ ohms, and varous other parameters. For instance, Schelkunoff[2] gives for the Q of a pill-box resonator

$$Q = \frac{1.20(\sqrt{\mu/\epsilon}/R)}{1 + a/h} \tag{5.39}$$

Here a is the radius of the resonator and h is the height. If we express the radius in terms of the resonant wavelength λ_0 ($a = 1.2\lambda_0/\pi$), we obtain

$$Q = \frac{\pi(\sqrt{\mu/\epsilon}/R)(v/c)}{(1 + h/a)n} \tag{5.40}$$

Here n is the number of resonators per wavelength (assuming the walls separating the resonators to be of negligible thickness); thus

$$n = h/\lambda = (h/\lambda_0)(c/v) \tag{5.41}$$

From (5.40) and (5.38) we obtain for a series of pill-box resonators

$$\text{db/wavelength} = 8.68(R/\sqrt{\mu/\epsilon})(c/v_g)(1 + h/a)n \tag{5.42}$$

In Appendix III an estimate of the Q of an array of fine half-wave parallel wires is made by assuming conduction in one direction with a surface resistance R. On this basis, Q is found to be

$$Q = (\sqrt{\mu/\epsilon}/R)(v/c) \tag{5.43}$$

and hence

$$\text{db/wavelength} = 27.3(R/\sqrt{\mu/\epsilon})(c/v_g) \tag{5.44}$$

For non-magnetic materials, surface resistance varies as the square root of the resistivity times the frequency. The table below gives R for copper and db/wavelength for pill-box resonators for $h/a \ll 1$ (5.42) and for wires (5.44) for several frequencies

f, mc	R, Ohms	(db/wavelength)/ (c/v_g)	
		Pill-box Resonators	Wires
3,000	.0142	$3.3 \times 10^{-4}n$	10.3×10^{-4}
10,000	.0260	$6.0 \times 10^{-4}n$	18.1×10^{-4}
30,000	.0450	$10.4 \times 10^{-4}n$	32.6×10^{-4}

In Section 3.3b a circuit made up of resonators, with a group velocity .031 times the phase velocity, was discussed. Suppose such a circuit were

[2] Electromagnetic Waves, S. A. Schelkunoff, Van Nostrand, 1943. Page 269.

used at 1,000 volts ($c/v = 16.5$), were 40 wavelengths long, and had three copper resonators per wavelength. The total attenuation in db is given below

f, mc	Attenuation, db
3,000	21
10,000	38
30,000	67

CHAPTER VI

THE CIRCUIT DESCRIBED IN TERMS OF NORMAL MODES

Synopsis of Chapter

IN CHAPTER II, the field produced by the current in the electron stream, which was assumed to vary as exp $(-\Gamma z)$, was deduced from a simple model in which the electron stream was assumed to be very close to an artificial line of susceptance B and reactance X per unit length. Following these assumptions, the voltage per unit length was found to be that of equation (2.10) and the field E in the z direction would accordingly be Γ times this, or

$$E = \frac{\Gamma^2 \Gamma_1 K}{\Gamma_1^2 - \Gamma^2} i \tag{6.1}$$

Here we will remember that Γ_1 is the natural propagation constant of the line, and K is the characteristic impedance.

We further replaced K by a quantity

$$E^2/\beta^2 P = 2K \tag{6.2}$$

where E is the field produced by a power flow P, and β is the phase constant of the line. For a lossless line, Γ_1 is a pure imaginary and

$$\beta^2 = -\Gamma_1^2 \tag{6.3}$$

From (6.1) and (6.2) we obtain

$$E = \frac{\Gamma^2 \Gamma_1 (E^2/\beta^2 P)}{2(\Gamma_1^2 - \Gamma^2)} i \tag{6.4}$$

To the writer it seems intuitively clear that the derivation of Chapter II is correct for waves with a phase velocity small compared with the velocity of light, and that (6.4) correctly gives the part of the field associated with the excitation of the circuit. However, it is clear that there are other field components excited; a bunched electron stream will produce a field even in the absence of a circuit. Further, many legitimate questions can be raised. For instance, in Chapter II capacitive coupling only was considered. What about mutual inductance between the electron stream and the inductances of the line?

The best procedure seems to be to analyze the situation in a way we know to be valid, and then to make such approximations as seem reasonable. One approximation we can make is, for instance, that the phase velocity of the wave is quite small compared with the speed of light, so that

$$| \Gamma_1 |^2 \gg \beta_0^2 = (\omega/c)^2 \tag{6.5}$$

In this chapter we shall consider a lossless circuit which supports a group of transverse magnetic modes of wave propagation. The finned structure of Fig. 4.3 is such a circuit, and so are the circuits of Figs. 4.8 and 4.9 (assuming that the fins are so closely spaced that the circuit can be regarded as smooth). It is assumed that waves are excited in such a circuit by a current in the z direction varying with distance as $\exp(-\Gamma z)$ and distributed normal to the z direction as a function of x and y, $\hat{J}(x, y)$. Such a current might arise from the bunching at low signal levels of a broad beam of electrons confined by a strong magnetic field so as not to move appreciably normal to the z direction.

The structure considered may support transverse electric waves, but these can be ignored because they will not be excited by the impressed current.

In the absence of an impressed current, any field distribution in the structure can be expressed as the sum of excitations of a number of pairs of normal modes of propagation. For one particular pair of modes, the field distribution normal to the z direction can be expressed in terms of a function $\hat{\pi}_n(x, y)$ and the field components will vary in the z direction as $\exp(\pm\Gamma_n z)$. Here the $+$ sign gives one mode of the pair and the $-$ sign the other. If Γ_n is real the mode is *passive*; the field decays exponentially with distance. If Γ_n is imaginary the mode is *active*; the field pattern of the mode propagates without loss in the z direction.

An impressed current which varies in the z direction as $\exp(-\Gamma z)$ will excite a field pattern which also varies in the z direction as $\exp(-\Gamma z)$, and as some function of x and y normal to the z direction. We may, if we wish, regard the variation of the field normal to the z direction as made up of a combination of the field patterns of the normal modes of propagation, the patterns specified by the functions $\hat{\pi}_n(x, y)$. Now, a pattern specified by $\hat{\pi}_n(x, y)$ coupled with a variation $\exp(\pm\Gamma_n z)$ in the z direction satisfies Maxwell's equations and the boundary conditions imposed by the circuit with *no* impressed current. If, however, we assume the same variation with x and y but a variation as $\exp(-\Gamma z)$ with z, Maxwell's equations will be satisfied only if there is an impressed current having a distribution normal to the z direction which also can be expressed by the function $\hat{\pi}_n(x, y)$.

Suppose we add up the various forced modes in such relative strength and phase that the total of the impressed currents associated with them is equal to the actual impressed current. Then, the sum of the fields of these

modes is the actual field produced by the actual impressed current. The field is so expressed in (6.44) where the current components J_n are defined by (6.36).

If it is assumed that there is only one mode of propagation, and if it is assumed that the field is constant over the electron flow, (6.44) can be put in the form shown in (6.47). For waves with a phase velocity small compared with the velocity of light, this reduces to (6.4), which was based on the simple circuit of Fig. 2.3.

Of course, actual circuits have, besides the one desired active mode, an infinity of passive modes and perhaps other active modes as well. In Chapter VII a way of taking these into account will be pointed out.

Actual circuits are certainly not lossless, and the fields of the helix, for instance, are not purely transverse magnetic fields. In such a case it is perhaps simplest to assume that the modes of propagation exist and to calculate the amount of excitation by energy transfer considerations. This has been done earlier[1], at first subject to the error of omitting a term which later[2] was added. In (6.55) of this chapter, (6.44) is reexpressed in a form suitable for comparison with this earlier work, and is found to agree.

Many circuits are not smooth in the z direction. The writer believes that usually small error will result from ignoring this fact, at least at low signal levels.

6.1 Excitation of Transverse Magnetic Modes of Propagation by a Longitudinal Current

We will consider here a system in which the natural modes of propagation are transverse magnetic waves. The circuit of Fig. 4.3, in which a slow wave is produced by finned structures, is an example. We will remember that the modes of propagation derived in Section 4.1 of Chapter IV were of this type. We will consider here that any structure the circuit may have (fins, for instance) is fine enough so that the circuit may be regarded as smooth in the z direction.

Any transverse electric modes which may exist in the structure will not be excited by longitudinal currents, and hence may be disregarded.

The analysis presented here will follow Chapter X of Schelkunoff's Electromagnetic Waves.

The divergence of the magnetic field H is zero. As there is no z component of field, we have

[1] J. R. Pierce, "Theory of the Beam-Type Traveling-Wave Tube," *Proc. I.R.E.*, Vol. 35, pp. 111–123, February, 1947.

[2] J. R. Pierce, "Effect of Passive Modes in Traveling-Wave Tubes," *Proc. I.R.E.*, Vol. 36, pp. 993–997, August, 1948.

$$\frac{\partial H_x}{\partial x} + \frac{\partial H_y}{\partial y} = 0 \tag{6.6}$$

This will be satisfied if we express the magnetic field in terms of a "stream function", π

$$H_x = \frac{\partial \pi}{\partial y} \tag{6.7}$$

$$H_y = -\frac{\partial \pi}{\partial x} \tag{6.8}$$

π can be identified as the z component of the vector potential (the vector potential has no other components).

We will assume π to be of the form

$$\pi = \hat{\pi}\,(x, y)e^{-\Gamma z} \tag{6.9}$$

Here $\hat{\pi}\,(x, y)$ is a function of x and y only, which specifies the field distribution in any x, y plane.

We can apply Maxwell's equations to obtain the electric fields

$$\frac{\partial H_z}{\partial y} - \frac{\partial H_y}{\partial z} = j\omega\epsilon E_x$$

Using (6.7) and (6.8), and replacing differentiation with respect to z by multiplication by $-\Gamma$, we find

$$E_x = \frac{j\Gamma}{\omega\epsilon}\frac{\partial \pi}{\partial x} \tag{6.10}$$

Similarly

$$E_y = \frac{j\Gamma}{\omega\epsilon}\frac{\partial \pi}{\partial y} \tag{6.11}$$

We see that in an x, y plane, a plane perpendicular to the direction of propagation, the field is given as the gradient of a scalar potential V

$$V = (-j\Gamma/\omega\epsilon)\pi \tag{6.12}$$

This is because we deal with transverse magnetic waves, that is, with waves which have no longitudinal or z component of magnetic field. Thus, a closed path in an x, y plane, which is normal to the direction of propagation, will link no magnetic flux, and the integral of the electric field around such a path will be zero.

We can apply the curl relation and obtain E_z

$$\begin{aligned} \frac{\partial H_y}{\partial x} - \frac{\partial H_x}{\partial y} &= j\omega\epsilon E_z \\ E_z &= \frac{j}{\omega\epsilon}\left(\frac{\partial^2 \pi}{\partial x^2} + \frac{\partial^2 \pi}{\partial y^2}\right) \end{aligned} \tag{6.14}$$

Applying Maxwell's equations again, we have

$$\frac{\partial E_z}{\partial y} - \frac{\partial E_y}{\partial z} = j\omega\mu H_x$$

$$\frac{j}{\omega\epsilon}\frac{\partial}{\partial y}\left(\frac{\partial^2\hat{\pi}}{\partial x^2} + \frac{\partial^2\hat{\pi}}{\partial y^2}\right) + \frac{j\Gamma^2}{\omega\epsilon}\frac{\partial\hat{\pi}}{\partial y} = -j\omega\mu\frac{\partial\hat{\pi}}{\partial y} \tag{6.15}$$

This is certainly true if

$$\frac{\partial^2\hat{\pi}}{\partial x^2} + \frac{\partial^2\pi}{\partial y^2} = -(\Gamma^2 + \beta_0^2)\hat{\pi} \tag{6.16}$$

$$\beta_0 = \omega\sqrt{\mu\epsilon} = \omega/c \tag{6.17}$$

We find that this satisfies the other curl E relations as well.

From (6.16) and (6.14) we see that

$$E_z = (-j/\omega\epsilon)(\Gamma^2 + \beta_0^2)\hat{\pi}(x, y)e^{-\Gamma z} \tag{6.18}$$

For a given physical circuit, it will be found that there are certain real functions $\hat{\pi}_n(x, y)$ which are zero over the conducting boundaries of the circuit, assuring zero tangential field at the surface of the conductor, and which satisfy (6.16) with some particular value of Γ, which we will call Γ_n. Thus, as a particular example, for a square waveguide of width W some (but not all) of these functions are

$$\hat{\pi}_n(x, y) = \cos(n\pi y/W)\cos(n\pi x/W) \tag{6.19}$$

where n is an integer. We see from (6.10), (6.11) and (6.18) that this makes E_x, E_y and E_z zero at the conducting walls $x = \pm W/2$, $y = \pm W/2$.

Each possible real function $\hat{\pi}_n(x, y)$ is associated with two values of Γ_n, one the negative of the other. The Γ_n's are the natural propagation constants of the normal modes, and the $\hat{\pi}_n$'s are the functions giving their field distribution in the x, y plane. The $\hat{\pi}_n$'s can be shown to be orthogonal, at least in typical cases. That is, integrating over the region in the x, y plane in which there is field

$$\iint \hat{\pi}_n(x, y)\,\hat{\pi}_m(x, y)\,dx\,dy = 0$$

$$n \neq m \tag{6.20}$$

For a lossless circuit the various field distributions fall into two classes: those for which Γ_n is imaginary, called active modes, which represent waves which propagate without attenuation; and those for which Γ_n is real, which change exponentially with amplitude in the z direction but do not change in phase. The latter can be used to represent the disturbance in a waveguide below cutoff frequency, for instance.

If Γ_n is imaginary (an active mode) the power flow is real, while if Γ_n is real (a passive mode) the power flow is imaginary (reactive or "wattless" power).

The spatial distribution functions $\hat{\pi}_n$ and the corresponding propagation constants Γ_n are a means for specifying the electrical properties of a physical structure, just as are the physical dimensions which describe the physical structure and determine the various $\hat{\pi}_n$'s and Γ_n's. In fact, if we know the various π_n's and Γ_n's, we can determine the response of the structure to an impressed current without direct reference to the physical dimensions.

In terms of the $\hat{\pi}_n$'s and Γ_n's, we can represent any unforced disturbance in the circuit in the form

$$\sum_n \hat{\pi}_n(x, y)[A_n e^{-\Gamma_n z} + B_n e^{\Gamma_n z}] \tag{6.21}$$

Here A_n is the complex amplitude of the wave of the nth spatial distribution traveling to the right, and B_n the complex amplitude of the wave of the same spatial distribution traveling to the left.

It is of interest to consider the power flow in terms of the amplitude, A_n or B_n. We can obtain the power flow P by integrating the Poynting vector over the part of the x, y plane within the conducting boundaries

$$\begin{aligned} P &= \frac{1}{2}\int\int EXH^* \, ds \\ P &= \frac{1}{2}\int\int (E_x H_y^* - E_y H_x^*) \, dx \, dy \end{aligned} \tag{6.22}$$

By expressing the fields in terms of the stream function, we obtain

$$P = A_n A_n^* \left(\frac{-j\Gamma_n}{2\omega\epsilon}\right) \iint \left[\left(\frac{\partial \hat{\pi}_n}{\partial x}\right)^2 + \left(\frac{\partial \hat{\pi}_n}{\partial y}\right)^2\right] dx \, dy \tag{6.23}$$

We can transform this by integrating by parts (essentially Green's theorem). Thus

$$\int_{x_1}^{x_2} \frac{\partial \hat{\pi}_n}{\partial x} \frac{\partial \hat{\pi}_n}{\partial x} \, dx = \hat{\pi}_n \frac{\partial \hat{\pi}_n}{\partial x}\Bigg|_{x_1}^{x_2} - \int_{x_1}^{x_2} \hat{\pi}_n \frac{\partial^2 \hat{\pi}_n}{\partial x^2} \, dx \tag{6.24}$$

Here x_1 and x_2, the limits of integration, lie on the conducting boundaries where $\hat{\pi}_n = 0$, and hence the first term on the right is zero. Doing the same for the second term in (6.23), we obtain

$$P_n = A_n A_n^* \left(\frac{-j\Gamma_n}{2\omega\epsilon}\right) \iint \hat{\pi}_n \left(\frac{\partial^2 \hat{\pi}_n}{\partial x^2} + \frac{\partial^2 \hat{\pi}_n}{\partial y^2}\right) dx \, dy \tag{6.25}$$

By using (6.16), we obtain

$$P_n = A_n A_n^* \left(\frac{j\Gamma_n}{2\omega\epsilon}\right)(\Gamma_n^2 + \beta_0^2) \iint (\hat{\pi}_n)^2 \, dx \, dy \tag{6.26}$$

It is also of interest to express the z component of the nth mode, E_{zn}, explicitly. For the wave traveling to the right we have, from (6.18),

$$E_{zn} = A_n \left(\frac{-j}{\omega\epsilon}\right)(\Gamma_n^2 + \beta_0^2)\hat{\pi}_n(x, y) \tag{6.27}$$

Let the field at some particular position, say, $x = y = 0$, be E_{zn0}. Then

$$A_n = \frac{j\omega\epsilon E_{zn0}}{(\Gamma_n^2 + \beta_0^2)\,\hat{\pi}_n(0, 0)} \tag{6.28}$$

and from (6.26)

$$P_n = (E_{zn0} E_{zn0}^*) \frac{-j\omega\epsilon\Gamma_n}{2\hat{\pi}_n^2(0, 0)(\Gamma_n^2 + \beta_0^2)} \iint [\hat{\pi}_n(x, y)]^2 \, dx \, dy \tag{6.29}$$

We can rewrite this

$$\frac{E_{zn0} E_{zn0}^*}{(-\Gamma_n^2)P_n} = \frac{2\hat{\pi}_n^2(0, 0)(\Gamma_n^2 + \beta_0^2)}{-j\omega\epsilon\Gamma_n(-\Gamma_n^2) \iint [\hat{\pi}_n(x, y)]^2 \, dx \, dy} \tag{6.30}$$

For an active mode in a lossless circuit, Γ_n is a pure imaginary, and the negative of its square is the square of the phase constant. Thus, for a particular mode of propagation we can identify (6.30) with the circuit parameter $E^2/\beta^2 P$ which we used in Chapter II.

Let us now imagine that there is an impressed current J which flows in the z direction and has the form

$$J = \hat{J}(x, y)e^{-\Gamma z} \tag{6.31}$$

According to Maxwell's equations we must have

$$\frac{\partial H_y}{\partial x} - \frac{\partial H_x}{\partial y} = j\omega\epsilon E_z + J \tag{6.32}$$

Now, we will assume that the fields are given by some overall stream function π which varies with x and y and with z as $\exp(-\Gamma z)$.

In terms of this function π, H_x, H_y and E_x, E_y will be given by relations (6.7), (6.8), (6.10), (6.11). However, the relation used in obtaining E_z is not valid in the presence of the convection current. Instead of (6.16) we have

$$\begin{aligned} \frac{\partial H_y}{\partial x} - \frac{\partial H_x}{\partial y} &= j\omega\epsilon E_z + J \\ E_z &= \frac{j}{\omega\epsilon}\left(\frac{\partial^2\pi}{\partial x^2} + \frac{\partial^2\pi}{\partial y^2}\right) + \frac{j}{\omega\epsilon} J \end{aligned} \tag{6.33}$$

Again applying the relation

$$\frac{\partial E_z}{\partial y} - \frac{\partial E_y}{\partial z} = -j\omega\mu H_x$$

we obtain

$$\frac{\partial^2 \pi}{\partial x^2} + \frac{\partial^2 \pi}{\partial y^2} = -(\Gamma^2 + \beta_0^2)\,\pi - J \tag{6.34}$$

We will now divide both π and J into the spatial distributions characteristic of the normal unforced modes.
Let

$$\hat{J}(x, y) = \sum_n J_n \hat{\pi}_n(x, y) \tag{6.35}$$

$$J_n = \frac{\iint \hat{J}(x, y)\hat{\pi}_n(x, y)\,dx\,dy}{\iint [\hat{\pi}_n(x, y)]^2\,dx\,dy} \tag{6.36}$$

This expansion is possible because the π_n's are orthogonal. Let

$$\hat{\pi} = e^{-\Gamma z} \sum_n C_n \hat{\pi}_n(x, y) \tag{6.37}$$

Here there is no question of forward and backward waves; the forced excitation has the same z-distribution as the forcing current.

For the nth component, we have, from (6.16),

$$\frac{\partial^2 \hat{\pi}_n(x, y)}{\partial x^2} + \frac{\partial^2 \hat{\pi}_n(x, y)}{\partial y^2} = -(\Gamma_n^2 + \beta_0^2)\hat{\pi}_n(x, y) \tag{6.38}$$

From (6.34) we must also have

$$C_n\left(\frac{\partial^2 \hat{\pi}_n(x, y)}{\partial x^2} + \frac{\partial^2 \hat{\pi}_n(x, y)}{\partial y^2}\right) = -C_n(\Gamma^2 + \beta_0^2)\hat{\pi}_n(x, y) - J_n \hat{\pi}_n(x, y) \tag{6.39}$$

Accordingly, we must have

$$C_n = \frac{J_n}{\Gamma_n^2 - \Gamma^2} \tag{6.40}$$

The overall stream function is thus

$$\pi = e^{-\Gamma z} \sum_n \frac{\hat{\pi}_n(x, y) J_n}{\Gamma_n^2 - \Gamma^2} \tag{6.41}$$

From (6.33) and (6.34) we see that

$$E_z = \frac{-j}{\omega\epsilon}(\Gamma^2 + \beta_0^2)\pi \tag{6.42}$$

So

$$E_z = e^{-\Gamma z} \sum \frac{-j(\Gamma^2 + \beta_0^2)\hat{\pi}_n(x, y)J_n}{\omega\epsilon(\Gamma_n^2 - \Gamma^2)} \tag{6.43}$$

$$E_z = \frac{-j(\Gamma^2 + \beta_0^2)}{\omega\epsilon} e^{-\Gamma z} \sum \frac{\hat{\pi}_n(x, y)J_n}{\Gamma_n^2 - \Gamma^2} \tag{6.44}$$

6.2 Comparison with Results of Chapter II

Let us consider a case in which there is only one mode of propagation, characterized by $\hat{\pi}_1(x, y)$, Γ_1, and a case in which the current flows over a region in which $\hat{\pi}_1(x, y)$ has a constant value, say, $\hat{\pi}_1(0, 0)$. This corresponds to the case of the transmission line which was discussed in Chapter II.

We take only the term with the subscript 1 in (6.44) and (6.30). Combining these equations, we obtain for the field at 0, 0

$$E_z = \frac{(E^2/\beta^2 P)(\Gamma^2 + \beta_0^2)}{(\Gamma_1^2 + \beta_0^2)} \frac{\Gamma_1^3 J_1 \iint [\hat{\pi}_1(x, y)]^2 \, dx \, dy}{2\hat{\pi}_1(0, 0)} \tag{6.45}$$

We have from (6.36)

$$J_1 = \frac{\pi_1(0, 0)}{\iint [\hat{\pi}_1(x, y)]^2 \, dx \, dy} \tag{6.46}$$

From (6.45) and (6.46) we obtain

$$E_z = \frac{(\Gamma^2 + \beta_0^2)\Gamma_1^3(E^2/\beta^2 P)}{2(\Gamma_1^2 + \beta_0^2)(\Gamma_1^2 - \Gamma^2)} Je^{-\Gamma z} \tag{6.47}$$

Let us compare this with (6.4), which came from the transmission line analogy of Chapter II, identifying E_z and J with E and i. We see that, for slow waves for which

$$\beta_0^2 \ll |\Gamma_1^2| \tag{6.48}$$

$$\beta_0^2 \ll |\Gamma^2| \tag{6.49}$$

(6.47) becomes the same as (6.4). It was, of course, under the assumption that the waves are slow that we obtained (2.10), which led to (6.4).

6.3 Expansion Rewritten in Another Form

Expression (6.44) can be rewritten so as to appear quite different. We can write

$$\Gamma^2 + \beta_0^2 = \Gamma^2 - \Gamma_n^2 + \Gamma_n^2 + \beta_0^2$$

Thus, we can rewrite the expression for E_z as

$$E_z = e^{-\Gamma z}\left((-j/\omega\epsilon)\sum_n \frac{(\Gamma_n^2 + \beta_0^2)\hat{\pi}_n(x, y)J_n}{\Gamma_n^2 - \Gamma^2} + (j/\omega\epsilon)\sum_n \hat{\pi}_n(x, y)J_n\right) \tag{6.50}$$

The second term in the brackets is just $j/\omega\epsilon$ times the impressed current, as we can see from (6.35). The first term can be rearranged

$$(-j/\omega\epsilon)(\Gamma_n^2 + \beta_0^2)J_n = \frac{(-j/\omega\epsilon)(\Gamma_n^2 + \beta_0^2)\iint \hat{\pi}_n(x, y)J(x, y)\,dx\,dy}{\iint [\hat{\pi}_n(x, y)]^2\,dx\,dy} \tag{6.51}$$

Referring back to (6.29), let Ψ_n be twice the power P_n carried by the unforced mode when the field strength is

$$|E_{zn0}| = 1 \tag{6.52}$$

Further, let us choose the $\hat{\pi}_n$'s so that, at some specified position, $x = y = 0$,

$$_n(0, 0) = 1 \tag{6.53}$$

Then

$$\Psi_n = \frac{-j\omega\epsilon\Gamma_n}{\Gamma_n^2 + \beta_0^2}\iint [\hat{\pi}_n(x, y)]^2\,dx\,dy \tag{6.54}$$

Using this in connection with (6.51), we obtain

$$E_z = e^{-\Gamma z}\left(-\sum_n \frac{\Gamma_n\hat{\pi}_n(x, y)\iint \hat{\pi}_n(x, y)\hat{J}(x, y)\,dx\,dy}{\Psi_n(\Gamma_n^2 - \Gamma^2)} + (j/\omega\epsilon)\hat{J}(x, y)\right) \tag{6.55}$$

An expression for the forced field in terms of the parameters of the normal modes was given earlier[1,2]. In deriving this expression, the existence of a set of modes was assumed, and the field at a point was found as an integral over the disturbances induced in the circuit to the right and to the left and propagated to the point in question. Such a derivation applies for lossy and mixed waves, while that given here applies for lossless transverse-magnetic waves only.

The earlier derivation[1] leads to an expression identical with (6.55) except that Ψ_n^* appears in place of Ψ_n. In this earlier derivation a sign was implicitly assigned to the direction of flow of reactive power (which really doesn't flow at all!) by saying that the reactive power flows in the direction in which the amplitude decreases. If we had assumed the reactive power to flow in the direction in which the amplitude increases, then, with the same definition of Ψ_n, for a passive mode Ψ_n^* would have been replaced by $-\Psi_n^*$ which is equal to Ψ_n (for a passive mode, Ψ_n is imaginary).

In deriving (6.55), no such ambiguity arose, because the power flow was identified with the complex Poynting vector for the particular type of wave considered. In any practical sense, Ψ is merely a parameter of the circuit, and it does not matter whether we call Im Ψ reactive power flow to the right or to the left.

The existence of a derivation of (6.55) not limited in its application to lossless transverse magnetic waves is valuable in that practical circuits often have some loss and often (in the case of the helix, for instance) propagate mixed waves.

6.4 Iterated Structures

Many circuits, such as those discussed in Chapter IV, have structure in the z direction. Expansions such as (6.55) do not strictly apply to such structures. We can make a plausible argument that they will be at least useful if all field components except one differ markedly in propagation constant from the impressed current. In this case we save the one component which is nearly in synchronism with the impressed current and hope for the best.

APPENDIX III

STORED ENERGIES OF CIRCUIT STRUCTURES

A3.1 Forced Sinusoidal Field

If $v \ll c$, the field can be very nearly represented inside the cylinder of radius a by

$$V = V_0 \frac{I_0(\beta r)}{I_0(\beta a)} e^{-j\beta z} = \frac{E}{j\beta} \frac{I_0(\beta r)}{I_0(\beta a)} e^{-j\beta z} \tag{1}$$

and outside by

$$V = V_0 \frac{K_0(\gamma r)}{K(\gamma a)} e^{-j\beta z} \tag{2}$$

Inside

$$\frac{\partial V}{\partial r} = \beta \frac{I_1(\beta r)}{I_0(\beta a)} e^{-j\beta z} V_0 \tag{3}$$

$$\frac{\partial V}{\partial z} = -j\beta \frac{I_0(\beta r)}{I_0(\beta a)} e^{-j\beta z} V_0 \tag{4}$$

Outside

$$\frac{\partial V}{\partial r} = -\beta \frac{K_1(\beta r)}{K_0(\beta a)} e^{-j\beta z} V_0 \tag{5}$$

$$\frac{\partial V}{\partial z} = -j\beta \frac{K_0(\beta r)}{K_0(\beta a)} e^{-j\beta z} V_0 \tag{6}$$

Because there is a sinusoidal variation in the z direction, the average stored electric energy per unit length will be

$$W_E = \left(\frac{1}{2}\right)\left(\frac{\epsilon}{2}\right) \int_{r=0}^{\infty} [(E_{r\,\max})^2 + (E_{z\,\max})^2](2\pi r\, dr) \tag{7}$$

Here $E_{r\ max}$ and $E_{z\ max}$ are maximum values at $r = a$. The total electric plus magnetic stored energy will be twice this. This gives

$$W = \frac{\pi\epsilon(\gamma a)^2}{2\gamma^2}\left[\frac{I_0^2 - I_0 I_2}{I_0^2} + \frac{K_0 K_2 - K_0^2}{K_0^2}\right] E^2$$

$$W = \frac{\pi\epsilon\gamma a}{\gamma^2}\left[\frac{I_1}{I_0} + \frac{K_1}{K_0}\right] E^2 \tag{8}$$

$$(E^2/\beta^2 P)^{1/3} = (c/v)^{1/3}(v/v_g)^{1/3}\left[\frac{120}{\beta a\left(\frac{I_1}{I_0} + \frac{K_1}{K_0}\right)}\right]^{1/3} \tag{9}$$

A3.2 Pill-Box Resonators

Schelkunoff gives on page 268 of Electromagnetic Waves an expression for the peak electric energy stored in a pill-box resonator, which may be written as

$$.135\ \pi\ \epsilon\ a^2 h E^2$$

Here a is the radius of the resonator and h is the axial length. For a series of such resonators, the peak stored electric energy per unit length, which is also the average electric plus magnetic energy per unit length, is

$$W = .135\ \pi\ \epsilon\ a^2 E^2 \tag{10}$$

For resonance

$$a = 1.2\lambda_0/\pi \tag{11}$$

Whence

$$W = .0618\ \epsilon\lambda_0^2 E^2 \tag{12}$$

And

$$(E^2/\beta^2 P)^{1/3} = 5.36\ (v/v_g)^{1/3}\ (v/c)^{1/3} \tag{13}$$

The case of square resonators is easily worked out.

A3.3 Parallel Wires

Let us consider very fine very closely spaced half-wave parallel wires with perpendicular end plates.

If z is measured along the wires, and y perpendicular to z and to the direction of propagation, the field is assumed to be

$$E_x = E\cos\beta x e^{\pm\beta y}\cos\frac{2\pi}{\lambda_0}z$$

$$E_y = E\sin\beta x e^{\pm\beta y}\cos\frac{2\pi}{\lambda_0}z \tag{14}$$

Here the + sign applies for $y < 0$ and the − sign for $y > 0$. We will then find that

$$W = 2W_E = \frac{\epsilon E^2 \lambda_0}{2} \int_0^\infty e^{-2\beta y}\, dy$$

$$W = \frac{\epsilon \lambda_0}{4\beta} E^2 \tag{15}$$

and

$$(E^2/\beta^2 P)^{1/3} = 6.20\ (v/v_g)^{1/3} \tag{16}$$

The surface charge density σ on one side of the array of wires (say, $y > 0$) is given by the y component of field at $y = 0$.

$$\sigma = \epsilon E_y = \epsilon E \sin \beta x \cos \frac{2\pi}{\lambda_0} z \tag{17}$$

This is related to the current I (flowing in the z direction) per unit distance in the x direction by

$$\frac{\partial I}{\partial z} = -\frac{\partial \sigma}{\partial t} \tag{18}$$

From (18) and (17) we obtain for the current on one side of the array

$$I = -\frac{j\omega\lambda_0 \epsilon}{2\pi} E \sin \beta x \sin \frac{2\pi}{\lambda_0} z \tag{19}$$

If we use the fact that $\omega\lambda_0/2\pi = c$ and $c\,\epsilon = 1/\sqrt{\mu/\epsilon}$, we obtain

$$I = \frac{-jE}{\sqrt{\mu/\epsilon}} \sin \beta x \sin \frac{2\pi}{\lambda_0} z \tag{20}$$

If R is the surface resistivity of either side ($y > 0$, $y < 0$) of the wires, when the wires act as a resonator (a standing wave) the average power lost per unit length for both sides is

$$P = \tfrac{1}{8} R \lambda_0 E^2/(\mu/\epsilon) \tag{21}$$

In this case the stored electric energy is half the value given by (15), and we find

$$Q = (\sqrt{\mu/\epsilon}/R)\ (v/c) \tag{22}$$